Analysis on Energy Balance for a Smart Grid in Stadshavens Area, Rotterdam

Lingxi Mi

Master of Science Thesis

TU Delft Delft University of Technology

Analysis on Energy Balance for a Smart Grid in Stadshavens Area, Rotterdam

Master of Science Thesis

For the degree of Master of Science in Electrical Engineering
Delft University of Technology

Lingxi Mi

January 26, 2012

· Faculty of Electrical Engineering, Mathematics and Computer Science
· Delft University of Technology

Abstract

Stadshavens, a 1600 hectares area of Rotterdam, appointed the next generation infrastructure to a plan on converting itself into an Eco-City. An important aspect of an Eco-City is involved in its electricity system. To meet the demands, an Eco-City requires the next generation electricity network, i.e., the Smart Grid.

In order to implement a smart grid for Stadshavens, the relationship of electricity supply and demand should be known and optimized by using a certain rule. As such, the objective of this thesis is aimed to conduct a feasibility analysis on a smart grid in the Stadshavens area.

Firstly, the energy demand was determined, by establishing the MATLAB model upon building type, the number of area and corresponding load curve and simulating. Thus, the amount of intuitive power consumption could be used for suitable selection of energy supply. Next, owing that the wind and solar were chosen as the source of the renewable energy in the place, the solar irradiance and wind speed were used to evaluate the energy potential. The solar production was calculated based on the restrictions of the proposed area and such optimal installing parameters and the wind energy production was calculated upon completion of height corrections. Then, the total maximum energy supply were obtained. Afterwards, the power flow balance regarding the energy demand and supply was investigated based on yearly changes in two scenarios (Green and Smart). By calculating the maximum energy production and the capacity of the storage system, it was found that the local power supply would meet the load demand only in spring and summer. This might be settled by extra power sources from other places. Also, the analysis on the cost was conducted to be used as the priority optimization standards. Finally, the electric vehicle, an indispensable element in a sustainable city, was introduced. By adjusting the charging time and method, it could reduce the power peak as well as smooth the power flow.

Table of Contents

List of Figures

List of Tables

Chapter 1

Introduction

1-1 Sustainable City

With the development of the modern society, tremendous cities established in the world. Accompanied with social changes, the cities encountered two major problems, i.e. the population explosion and energy shortage. As such, a sustainable city or eco-city was first coined by Richard Register as an ecologically healthy city in 1987[1]. It aimed to minimize the demand of energy, water, food or other necessities, and tended to reduce heat, air pollution - CO_2, methane, and water pollution, which can be more environment-friendly. As a result, a sustainable city can supply its own energy and food, minimize the dependence on the surrounding countryside, and assist the city residents in reducing the ecological footprint.

For example, Masdar City (UAE), the world's first planned carbon-neutral city, seeks to maximize the usage of renewable energy to maximize the carbon savings and the efficiency of the city's buildings and demand-side systems. In its first stage, it will construct a 60-megawatt photovoltaic power plant supplying the power for all construction activities. As well, additional photovoltaic modules capable of generating 130 megawatt (MW) will be placed based on stone-and-mud walls to provide the supplemental solar energy. Moreover, a 20 MW wind farm will be established outside the city's perimeter, intending to utilize geothermal power. Besides, a world's largest hydrogen power plant will be built as a part of the Masdar plan.

Promoting renewable energy and energy efficiency are related to not only the change in lifestyle, but also the technological innovation. Due to this sustainable philosophy, various means have been used, of which a sustainable energy infrastructure is critical to a high-class and high-tech eco-city. The next generation infrastructure addresses a sustainable, reliable and affordable energy system, including a smart electricity infrastructure.

1-2 Smart Grid

A smart electricity infrastructure or a smart grid is a new highly-integrated power grid based on the physical grid, shown in Figure 1-1. Similar to the existing grids, it possesses the capability of integrating such renewable electricity as solar and wind. It combines with the advanced sensor measurement technology, computer technology, information technology, control technology, communication technology and physical power.[2]

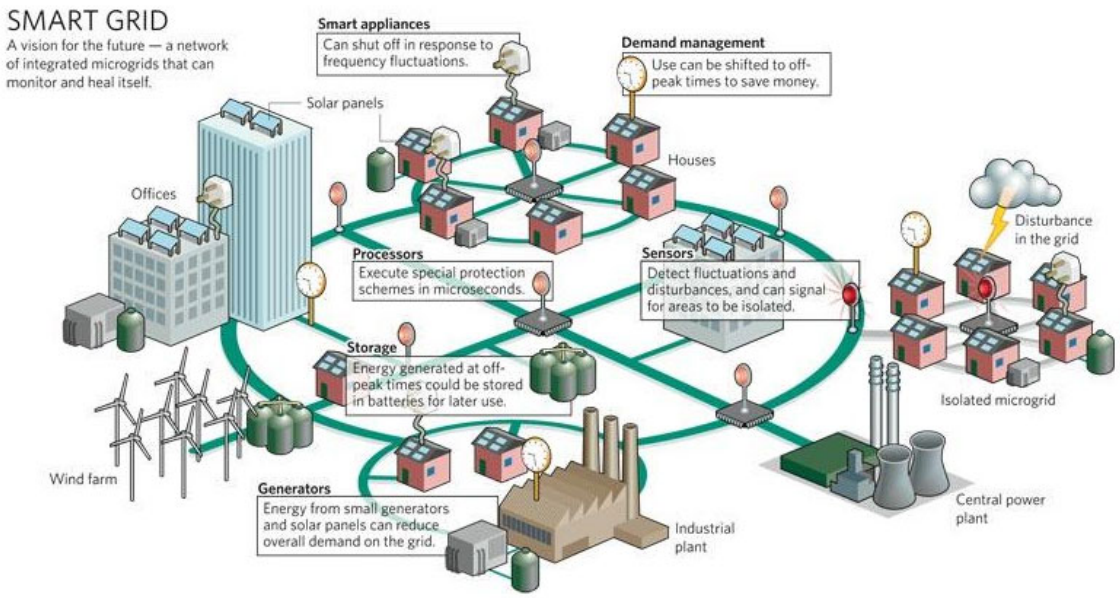

Figure 1-1: Smart grid concept, source: SIEMENS, a city of the future

To meet the user demand for electricity, the optimal allocation of resources and the requirements of environmental constraints should be considered. Once the power is least expensive, consumers can allow the smart grid to turn on the home appliances, whist the factories can undertake the production processes. At peak time, users can turn off some non-essential electrical appliances to reduce demand.

In addition, it ensures the power quality, reliability and economy of power supply, adapts the power market for the development purpose and achieves the electricity supply and value-added services for user clean, reliable and economical. Up to date, Smart grids are being promoted by many governments as a way of addressing energy independence, global warming and emergency resilience issues.

1-3 Research Goals

To follow the Masdar city as a pilot project, a number of cities in diverse countries subsequently run into action. In the Netherlands, Rotterdam as an active follower, intends to be a

trendsetter in the fields of sustainable energy. Stadshavens in Rotterdam with 1600 hectares plans itself as a energy neutral port area depending on its strategic location. It can provide people not only the necessities for their businesses, but also the residential environment along with cultural amenities and educational facilities.

In this study, the so-called DIEMIGO 2.0 Project was proposed to develop advanced and innovative technologies for renewable, alternative and sustainable energies (e.g. solar, wind, etc.), which assisted in building the first zero-carbon and zero-waste sustainable place in the Stadshavens area of Rotterdam.

The main goals of this thesis were aimed to make a feasibility analysis on matching the energy demand and supply in the area. Based on this notion, a prototype of smart gird could be designed. The solar and wind energy were used as the local energy source, possibly with a storage part to achieve a energy balance, and a charging system for sustainable mobility to improve the grid. To achieve these goals, following objectives were formulated:

· Analyzing the load demand and potential

It is to seek the load profile, solar irradiance and wind speed based on the database, to analysis the shape and distribution of the parametric curve and to ideally mix different loads and renewable sources of the area.

· Balancing the energy demand and supply

It is to match the energy as much as possible. The procedure is to determine the size of the solar panel and wind turbine, and to optimize the energy mixture to close to the energy neutral for the area using different strategies. After that, the cost is analyzed to determining the optimal scale of the supply.

· Adding a Electric Vehicle (EV) charging system

It is to build a charging system for the sustainable mobility. A smart charging strategy can be used to absorb the abundant energy, and to enhance the share of local energy utilized at the Stadshavens. It is a effective method to improve the grid.

1-4 Thesis Organization

This thesis contained five (5) chapters presented as follows.

The research method was developed in Chapter 2. This chapter was dedicated with background information about the smart grid and presentation of a generic design procedure for a

solar/wind system from each individual original data analysis, energy calculation to the final mixture of different load and renewable source.

In Chapter 3, the individual model of different load profiles and energy resources was first established to achieve the energy balance.Then, it presented the mixture of the energy demand and supply on the basis of the critical principle of energy balance and the power flow of the area. Different situations about the energy balance were analyzed with and without the battery storage system, and the cost analysis was used as an index for optimization.

The EV charging was discussed in Chapter 4. By choosing appropriate charging method and time, it can improve the grid and energy usage efficiency.

Chapter 5 provided the conclusions from this study the and recommendations on the future work.

Chapter 2

Methodology

2-1 Introduction

Unlike the regular power grid based on thermal power station, the smart grid will allow optimal usage of intermittent resources, such as solar and wind. They often reach their peak generating capacities during off-peak using hours. This will cause an energy redundancy in these cases. Such energy storage devices as batteries and new off-peak loads as electric vehicles, which reduce the overall energy redundancy and improve the electricity operation, are integrated in the smart grid[3].

Briefly, two impacts on electricity reliable for smart grid are involved.

- Imperative of energy balance, viz matching electricity production with demand.
- Stability of electricity operation, viz., the power flow will be as smooth as possible, so as for storage devices and electric vehicles to shift the power or load peak.

Based on these understandings, smart grid design and operation can be used to resolve these impacts. The developed methodology is described in steps.

2-2 Data Collection

The purpose of an energy balance is to satisfy energy consumption on a smaller scale. Since the energy demand and supply both are frequently changing, a regulation will be demanding on this variation. Thus, a real-time adjustment requires a complete availability of data[4]. In the other hand, the availability and magnitude of solar and wind energy is influenced by the climatic conditions, viz., a pre-feasibility analysis is necessary to investigate into weather data

of solar irradiance and wind speed for particular sites[5]. After dealing with the appropriate weather data required, the energy consumption or energy generated from a system can be calculated to design the system.

2-2-1 Climate Data

In this project, the local weather pattern is referred to the Royal Netherlands Meteorological Institute (KNMI). The KNMI provides relevant data in the Netherlands for the period 2001 to 2010, The values of solar irradiance and wind speed are recorded at a 10-minute interval. Such a large number of discrete values can hardly be displayed in the form of a curve regarding continuous time-scale. As such, a moving average is used to illustrate the trends on the solar irradiance and wind speed.

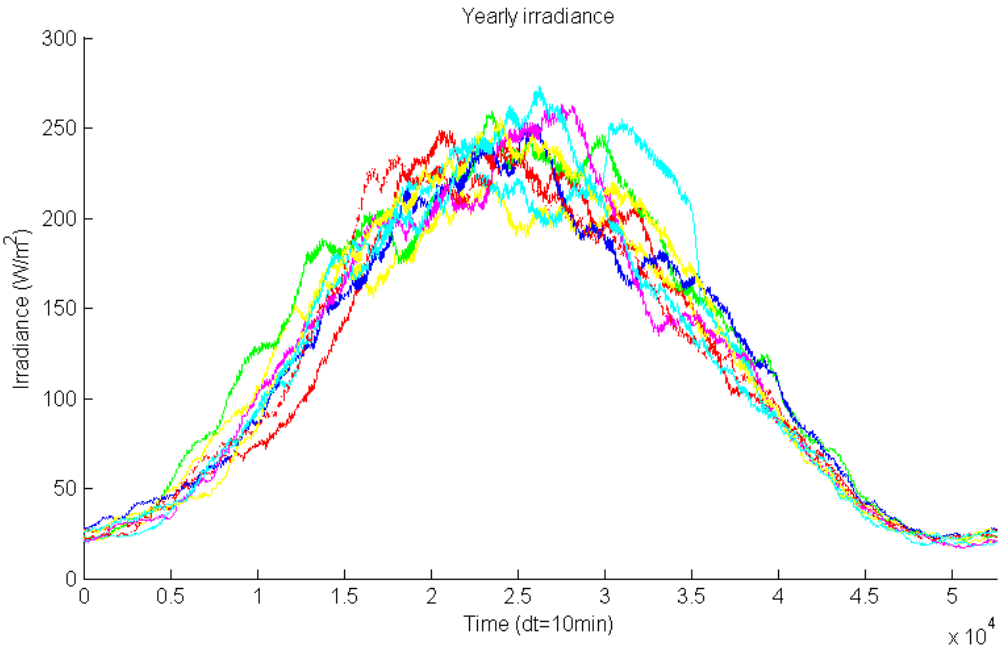

Figure 2-1: Smoothed yearly irradiance

Figure 2-1 shows the yearly moving average irradiance in the Netherlands during 2001 to 2010, except 2007 because of some monthly data missing. It is clearly indicated that the irradiance, like the temperature, reaches the peak in summer and goes to the bottom in the winter. Although the irradiance varies in a wide range (from 25 W/m^2 to 260 W/m^2), the variance among different years appears to be almost the same.

The wind speed was measured at a 10-meter height. Figure 2-2 exhibits the yearly moving average wind speed in the same condition. Unlike the solar irradiance, the annual differences are quite large, where the only regular pattern about the wind speed was detected higher in the cold days.

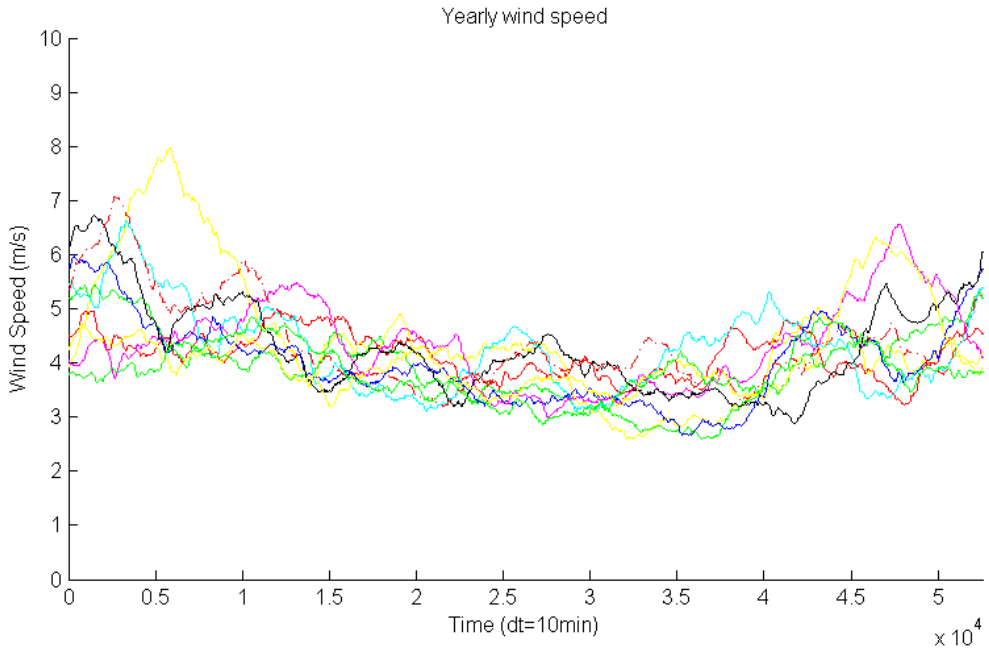

Figure 2-2: Smoothed yearly wind speed

Though the two figure above are not the real fluctuations of the solar irradiance and wind speed, it can still reflect the general trend of them, and can be used to calculate the energy output of the photovoltaic and wind turbine.

2-2-2 Load Data

For the profile of energy demand, only the typical Dutch households demand power in 2007 and 2008 are provided from Ecofys. But in this project, there are three different types of building, each of them is acquired via its different daily routine. The total load regarding the electric grid significantly varies over time. Although it is the sum of individual client choices, the overall load slowly changes in terms of average power consumption. As a result, the generalized electricity load profiles of diverse seasons for every building category should be clearly unveiled. Due to lack of the necessary information in the Netherlands, the real data measured in Norwegian are employed based on an assumption of a similar life habit[6][7].

House and Apartment Load

Previously, the houses and apartments are taken into account. The electrical loads of these buildings are obtained based on the use of common devices, such as electric stove, washing machine and water heater. By comparing results amongst surveys on the house electricity load in the Netherlands, the design load for house buildings is specified as follows[8].

- Electrical load during weekdays = 6.5 W/m^2
- Electrical load during weekends = 7.3 W/m^2

The generalized daily load profile for all seasons is provided in Figure 2-3.

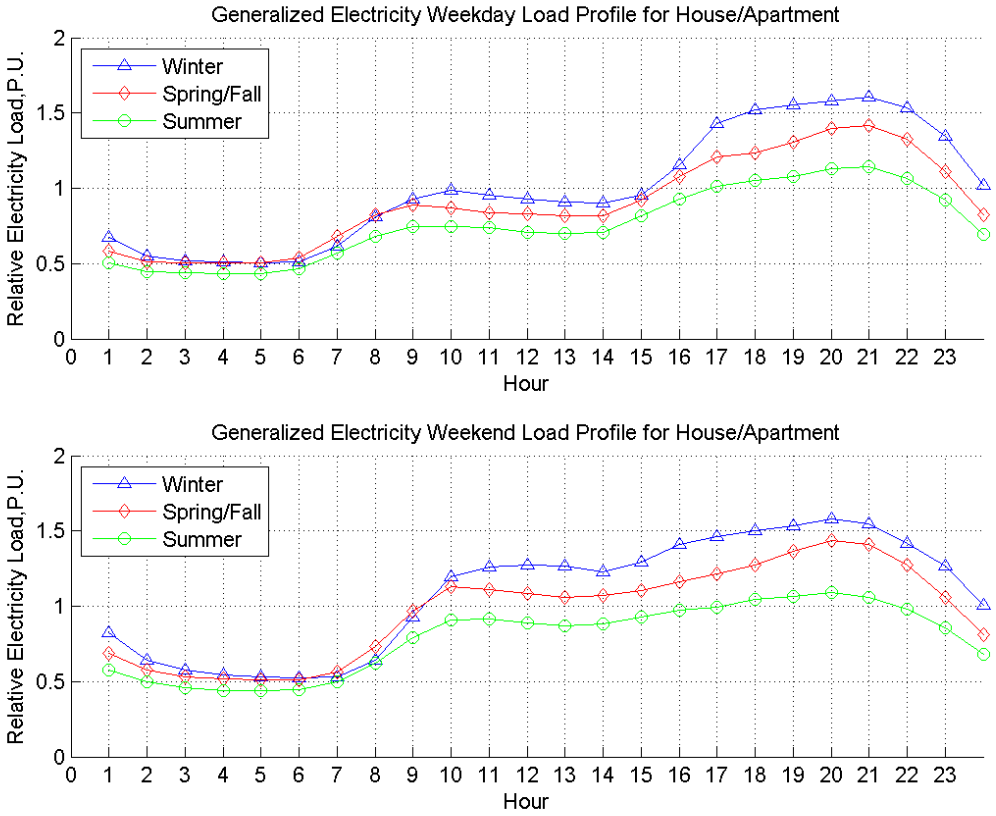

Figure 2-3: Generalized electricity load profiles, for all seasons for house

It is indicated that the difference between day and night time is more obvious in weekdays than in weekends due to working hours. The seasonal profiles are extremely similar during night hours for both day types. And the electricity load demand for winter is the highest. The weekly electricity load profiles of Stadshavens are estimated based on from the aforementioned data.

Amenity Load

Next, the amenity buildings are included. The load profile of amenity, including hotels, restaurants/bars, shops and co-coffees is studied. Particularly in the Netherlands, the design load for house buildings is specified as:

- Electrical load during weekdays = 6.3 W/m^2
- Electrical load during weekends = 6.7 W/m^2

The generalized daily load profile for all seasons is shown in Figure 2-4.

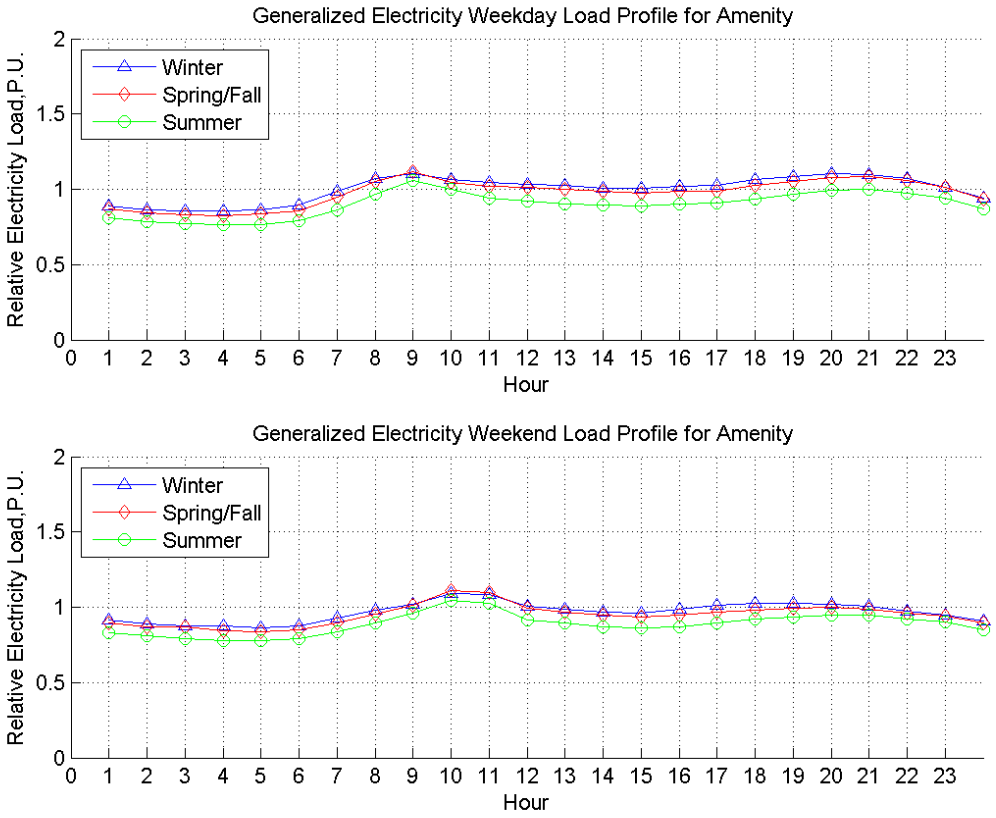

Figure 2-4: Generalized electricity load profiles, for all seasons for amenity

The winter and spring/fall electricity load profiles are quite similar in terms of size and shape for both day types, whilst the summer load profiles are slightly lower. Therein, the electricity demand in winter is still considered as the largest one. Subject to the daily variation, the electricity consumption reach the peaks twice in one day, viz., one to two hours after getting-up and the time duration from after-work to going-to-bed.

Office Load

Due that working is treated as one type of major activities in that area, so the load profile for office buildings is included. In this research, it is implied that the electricity load profile for office buildings is obtained based on the criterion of working hours. Referring to cases on the Netherlands, the design load for house buildings is specified as:

- Electrical load during weekdays = 12 W/m^2
- Electrical load during weekends = 6.6 W/m^2

Figure 2-5 illustrate the generalized electricity load profiles of office buildings for all seasons in weekdays and weekends, respectively.

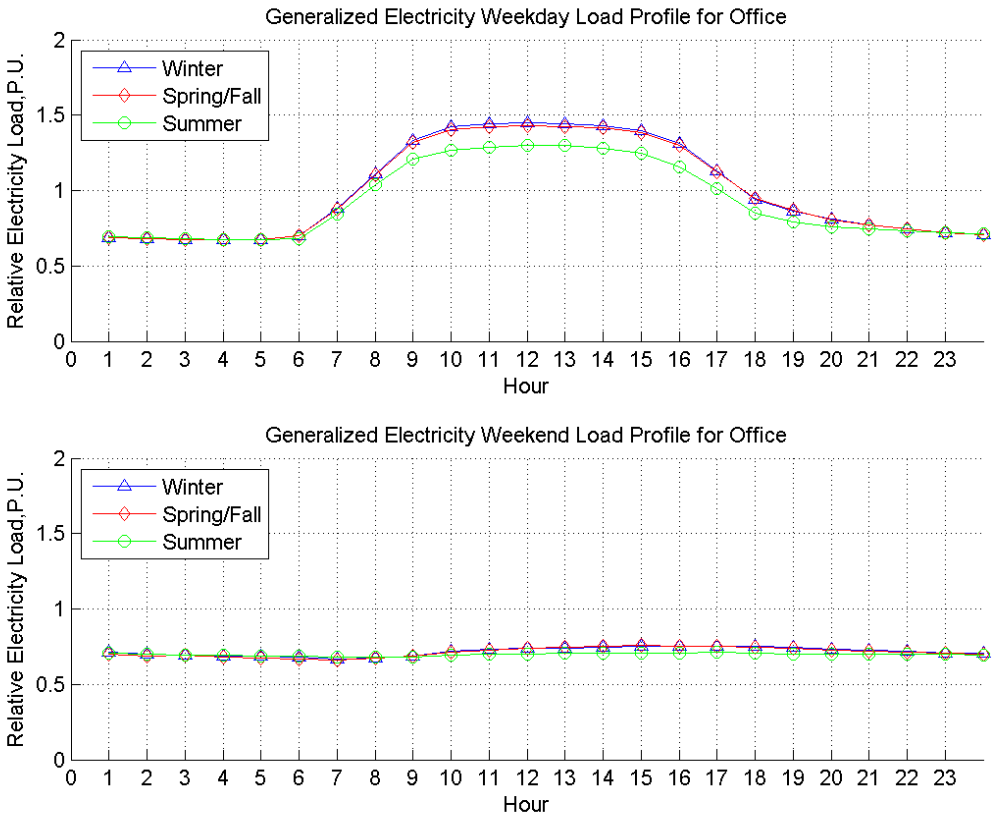

Figure 2-5: Generalized electricity load profiles, for all seasons for office

The winter and spring/fall electricity load profiles for weekdays are similar, but the summer profile display a bit higher load demand. The seasonal electricity load profiles in weekends slightly vary, because most of electricity consumption during this day type is of a standby variety.

2-3 Energy Calculation

The value of the energy demand can be directly got from the data provided, while the amount of energy supply should be calculated from the climate data and with some corrected.

Two categories of power generation (i.e. photovoltaic and wind turbine) are mutually complemented at the same time with regard to various features during energy collection, viz., the photovoltaic power generation possess reliable supply, low operation and maintenance fee; while the wind power generation have a high capacity, yet low reliability. The hybrid generation system can effectively improve the solar and wind power generation when a single output impact on power stability and reliability[9][10].

2-3-1 Solar Power Calculation

The solar power is the conversion of sunlight into electricity, proportional to the corresponding solar irradiance. Through the photovoltaic effect, solar panels can use light energy to generate electricity.

Obviously, the solar irradiance is abundant in spring and summer, and sufficient during daytime. They can be harvested to generate electricity by the means of photovoltaic systems. On the flat roofs, the photovoltaic modules will be frequently allocated in arrays in the optimized tilted position towards the sun. By calculating solar irradiance, the tilt of receiving surfaces deliver a great influence on energy yielding. Preventing arrays from reciprocal shading and avoiding arrays within a certain distance are considered with uncovered areas for maintenance (see Figure 2-6).

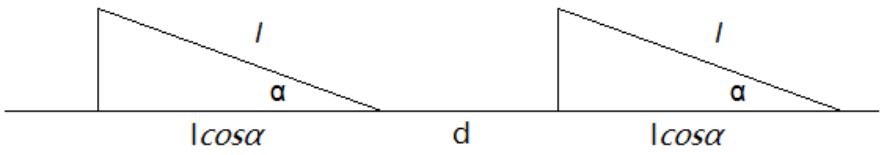

Figure 2-6: Ground cover ratio (GCR)

In general, a slight mismatch by the lowest solar radiation is unavoidable. By choosing an adequate Ground Cover Ratio (GCR)[11], it can be resolved. The ground cover ratio is defined by:

$$GCR = \frac{l}{d + l\cos\alpha} \tag{2-1}$$

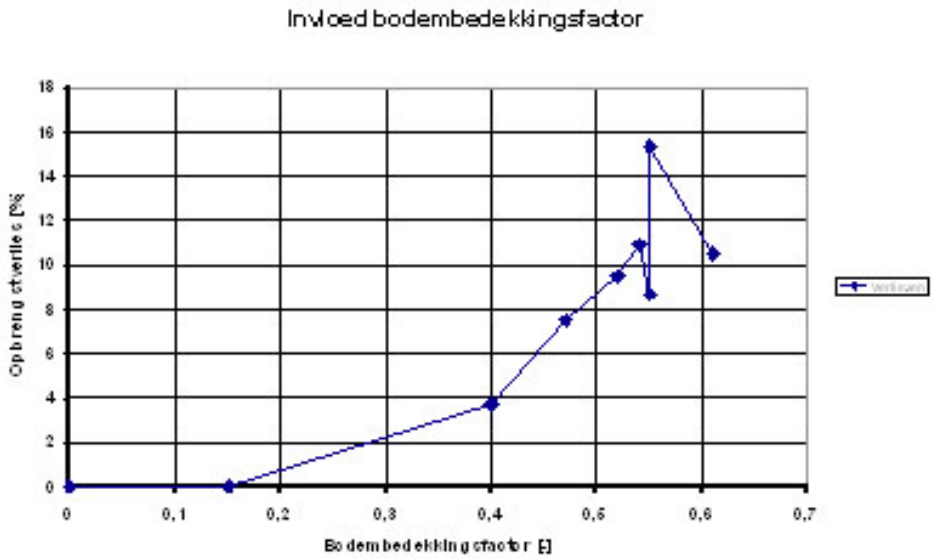

Figure 2-7: Distance between PV arrays and influence of the Ground Cover Ratio, source: www.pv-monitoring.novem.nl

In the Figure 2-7 shown above, the influence of the GCR on the annual mismatch is indicated. For example, a ground cover ratio of 50% produce an acceptable mismatch of 6%. And the optimized tilt angle α is 36°.

Since the KNMI data are measured from horizontal plane, it should be convert to the inclined plane. For solar irradiance on an inclined plane, it combines the direct beam, diffuse and reflected components. The total solar irradiance intercepts in one day H_α as[12]:

$$H_\alpha = H_b R_b + H_{d\alpha} + H_{g\alpha} \tag{2-2}$$

where H_b, $H_{d\alpha}$ and $H_{g\alpha}$ are the direct beam, diffuse and ground reflected irradiance respectively, and R_b is the ratio of the amount of the direct solar irradiance between inclined surface and the horizontal surface as:

$$R_b = \frac{cos(\phi-\alpha)cos\delta sin\omega_s^{'} + \pi\omega_s^{'} sin(\phi-\alpha)sin\delta/180}{cos\phi cos\delta sin\omega_s + \pi\omega_s sin\alpha sin\delta/180} \tag{2-3}$$

where ϕ is the latitude, δ is the solar declination which can be approximately expressed

$$\delta = -23.45°cos[360(10+n)/365] \tag{2-4}$$

where n is the day of the year beginning with Coordinated Universal Time's solar noon on January 1st as 0. $\omega_s^{'}$ and ω_s are the sunset hour angle on horizontal and tilt angle, for the northern hemisphere (ϕ>0), $\omega_s^{'}$=ω_s=cos^{-1}(-tgϕtgδ).

Assuming diffuse and reflected irradiance to be isotropic, the diffuse component can be expressed[13]

$$H_{d\alpha} = H_d(1 + cos\alpha)/2 \tag{2-5}$$

And the reflected component can be expressed

$$H_{g\alpha} = H\rho(1 - cos\alpha)/2 \tag{2-6}$$

where ρ is the ground reflectance, and approximate to be 0.2 on the land.

Since there are no diffuse irradiance data provided from KNMI, some approximate estimation is needed to get it. Under a standard clear sky, 23% of global irradiance is diffused[14]. The yearly converted solar irradiance is shown below.

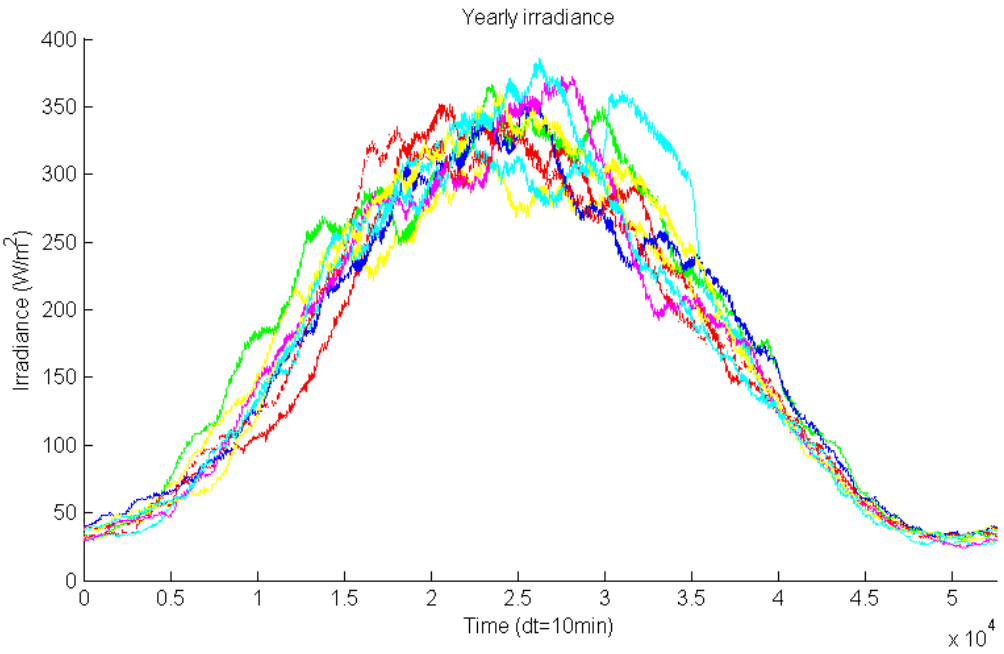

Figure 2-8: Smoothed yearly irradiance in 36° tilt angle

Coming to the commercial products, some electrical characteristics include nominal power (P_{MAX}, measured in W), peak power, kW_p, and module efficiency (%) should be considered.

2-3-2 Wind Power Calculation

The annual wind speed at a height of 10 meter is displayed in the former section, but the wind speed changes with height. To this end, the wind speed value should be corrected. The Hellman altitude formula is used for simple approximation[15], according to Equation 2-7,

where $v_{Wi,h}$ is the mean wind velocity at an altitude h and $v_{Wi,ref}$ is the wind speed at a reference altitude h_{ref} (mostly 10 m). α_{Hell} is the altitude wind exponent (i.e. Hellman-Exponent, the roughness exponent). A function of the roughness length and the thermal stability in the planetary boundary layer is presented as follows:

$$v_{Wi,h} = v_{Wi,ref}(\frac{h}{h_{ref}})\alpha_{Hell} \tag{2-7}$$

Table 2-1 shows approximate values of α_{Hell} in terms of near coastal surfaces and planetary boundary layers.

Table 2-1: Approximate values for the Hellman-Exponent

Stability	Open water surface	Flat,open coast	Cities, villages
Unstable	0.06	0.11	0.27
Neutral	0.10	0.16	0.34
Stable	0.27	0.40	0.60

Without the height restriction, wind speed at any height can be got. Based on the wind speed, the annual amount of energy produced by wind turbines is calculated[16].

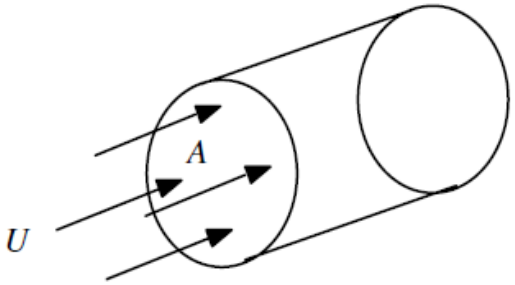

Figure 2-9: Flow of air through a rotor disk; A, area; U, wind velocity

From the continuity equation of fluid mechanics, the mass flow of air, dm/dt, through a rotor disk of area A is determined. As shown in Figure 2-9, the mass flow rate is expressed as a function of air density, ρ, and air velocity (assumed uniform), U, as follows:

$$\frac{dm}{dt} = \rho AU \tag{2-8}$$

The kinetic energy per unit time is depicted as:

$$P = \frac{1}{2}\frac{dm}{dt}U^2 = \frac{1}{2}\rho AU^3 \tag{2-9}$$

Possibly, a machine power curve is obtained via the wind power and the rotor power coefficient, C_p. The result is expressed in the following equation for P_w(U):

$$P_w(U) = \frac{1}{2}\rho A C_p \eta U^3 \tag{2-10}$$

where η is the train driven efficiency (i.e. generator power/rotor power), the air density is 1.225 kg/m^3 in standard conditions (i.e. sea-level, 15 °C). For idealized wind turbine with no losses, the machine power coefficient, C_p, is equal to the Betz limit, ($C_{p,Betz}$=16/27), and the Betz limit is supposed as the theoretical maximum possible power coefficient.

For the commercial product, every wind turbine has a characteristic power performance curve and the power output of a wind turbine varies with wind speed. Figure 2-10 presents an example of a power curve for a wind turbine.

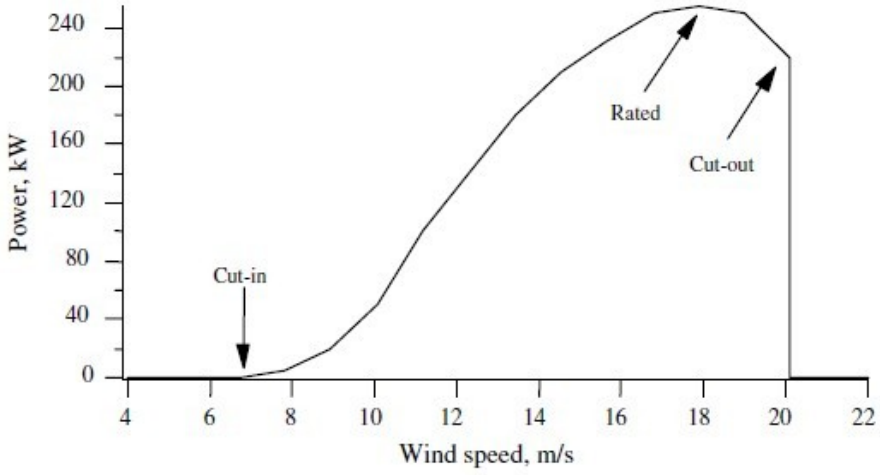

Figure 2-10: Typical wind turbine power curve, source: Wind Energy Explained

From Figure 2-10, three key points on the velocity scale are important.

- Cut-in speed: the minimum wind speed at which the machine will produce useful power.
- Rated wind speed: the wind speed at which the rated power (generally the maximum power output of the electrical generator) is reached.
- Cut-out speed: the maximum wind speed at which the turbine is allowed to deliver power.

2-4 Unit Sizing

The unit sizing for an integrated power system secures a crucial position in speculating the reliability and economy of the system. Upon completion of the pre-feasibility analysis, the selection of proper size of equipments is conducted based on weather data and maximum capacities[17].

2-4-1 Solar Panel Sizing

For solar panel, considering the GCR, only 35% of the surface area can be used to absorb the solar irradiance. For the module efficiency, the solar panel produced the best efficiency of 21% in commercial products in current. The efficiency is expected on a significant increase by 30% using the new design concept.

2-4-2 Wind Turbine Sizing

Specifically for this project, the average wind speed at Stadshavens is nearly 4.2 m/s at 10 m, and the wind power per unit area is approximately 30 W/m^2. Compared with sampled qualitative magnitude evaluations of the wind resource, it is clear that without the height restriction, a better evaluations of the wind resource can be completed in a higher place.

Over the past 25 years, the large commercial wind turbines increased from approximately 50 kW to 2 MW, followed by machines up to 5 MW under design, the size of which is illustrated in Figure 2-11.

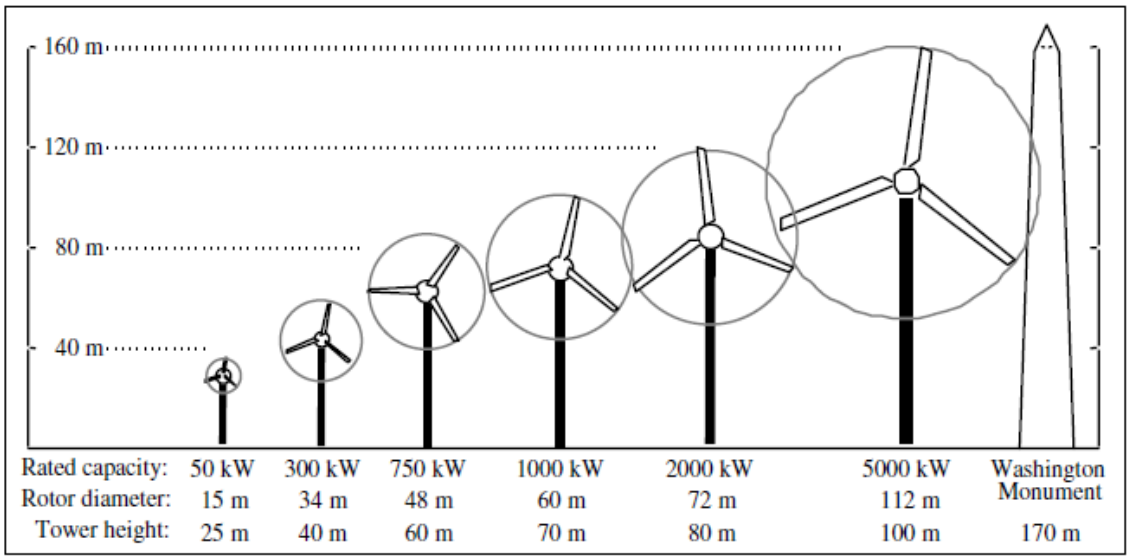

Figure 2-11: Representative size, height, and diameter of wind turbines, source: Wind Energy Explained

Subsequently, beside the large commercial wind turbines, small scale turbines are also available for residential scale use, especially be installed on a roof. These residential wind turbines produce a rate outputs of $2 - 10$ kW and they are usually approximately $2.1 - 7.6$ m in diameter.

By choosing a suitable wind turbine, the distribution position of wind turbine should be considered, because too dense layout can cause some problems. As a mitigation measure, a

minimum distance of 6 to 8 rotor diameter is applied as a rule of thumb between the wind turbine and the closest neighbor, which can reduce the effect of noisy and shadow flicker. And for wind turbines that are spaced 10 rotor diameters apart in the prevailing downwind direction and 5 rotor diameters apart in the crosswind direction, array losses can be decrease to less than 10%.

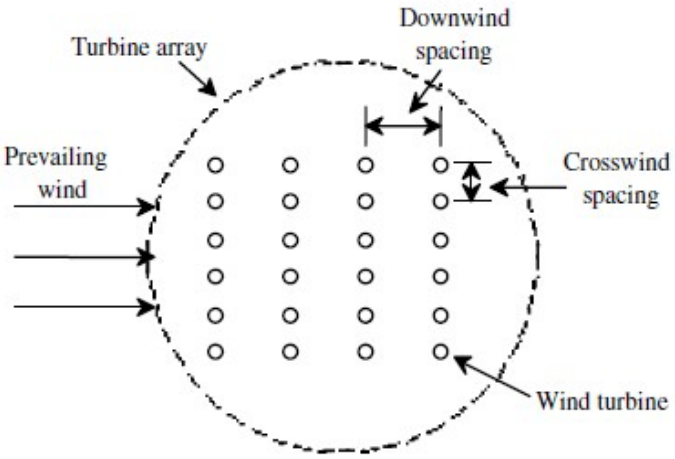

Figure 2-12: Wind farm array schematic, source: Wind Energy Explained

In this project two types of wind turbines can be installed : one is the large-scale wind turbine built on the ground. These wind turbines are built along the shore. As a height restriction of 60 m, the maximum size wind turbine used at this site is constrained to an axle height of 40 m and a rotor diameter of 34 m with a rated speed 13 m. The cut-in and cut-out speed are 3 m and 25 m, respectively. Referring the main wind direct in the Rotterdam, the interval between two wind turbine are approximately 170 m (5 rotor diameters). By considering the widths of specific rivers, utmost 24 wind turbines can be set up.

The other is the small-scale wind turbine built on the roof. Depending on the different definition of the urban scenario, which will be described in the next chapter. the maximum height of the building are assumed as 24 m (8 floors). In order to save the space, the vertical axis wind turbines are used, with the mounting height of 5.5 m at a rated speed 13 m. The rotor diameter and blade length are 3 m and 3.6 m respectively, which means the swept area is 10.6 m^2. The cut-in and cut-out speed are 3 m and 50 m, respectively.The ground space per wind turbine would be calculated as (10*3)*(5*3) = 450 m^2. The distribution position is similar in Figure 2-12.

Then the power per square meter between the solar panel and wind turbine are calculated and shown in Figure 2-13.

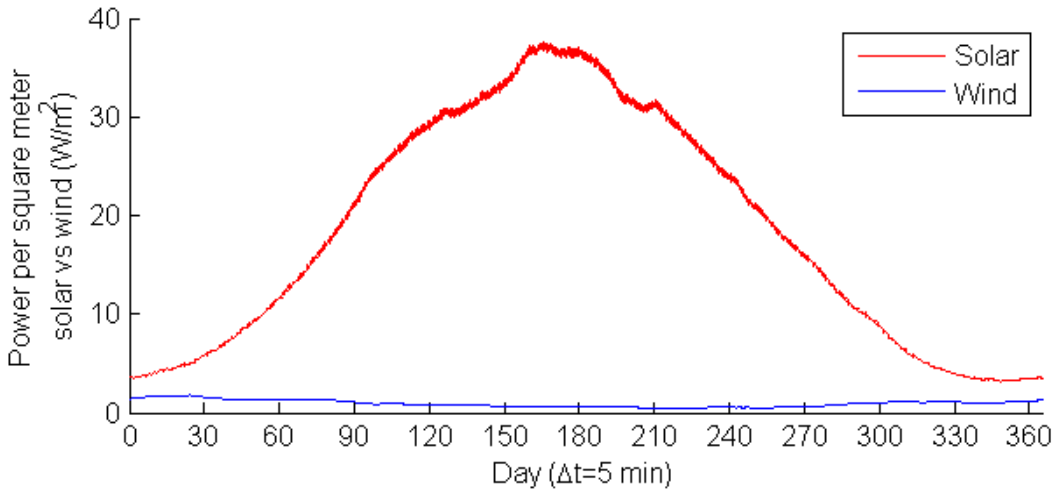

Figure 2-13: Power density between solar and wind

It is clear that the per square meter power generated from solar panel is higher than from the small scale wind turbine in all of the year. Since the solar panel and small wind turbine are alternative options built on the roof of building, it is preferred to choose the solar panel, which can produce more energy in the same area.

2-5 Energy Balance

Since the data of solar and wind energy are available for particular sites, an iterative algorithm is employed for determining the wind generator capacity and the number of solar panels for the smart grid system. The algorithm uses the actual wind speed, solar irradiance, and power demand to detect the solar/wind generation capacities as required. The statistical variation of energy supply is assumed as the battery storage[18]. Following operational strategies are employed[19]:

- The electric power generated by the solar panels and wind turbines is more precedent in satisfying electricity demand than that provided by batteries.
- If the total electric power generated by solar panels and wind turbines exceeds demands, the additional electric power will be charged into batteries.
- The remained electric power is recycled besides battery charging.
- If total electric power generated by solar panels and wind turbines is insufficient, the electric power will be discharged from batteries.
- If batteries cannot supply enough power, part of electric load should be shutdown from the electric power system or the extra generator backup is applied.

Based on abovementioned operational strategies, a power and energy balance for the proposed design should be undertaken[20]. Accordingly in an ideal balance, the total power in an integrated system is zero. Thus in the dynamic situation, the fraction of total power generated and demanded ΔP, is defined as

$$\Delta P = P_{gen} - P_{dem} \tag{2-11}$$

By considering the smooth operation, the gap between generated power, P_{gen}, and demanded power, P_{dem}, over a given period of time were minimized. The total average generated and demanded energies, i.e. W_{gen} and W_{dem}, within a day can be presented in terms of solar and wind power supply and the power demand as follows:

$$W_{gen} = \sum_{n=1}^{24} [(\Delta T)(N_w P(t)_w) + N_s P(t)_s] \tag{2-12}$$

$$W_{dem} = \sum_{n=1}^{24} [(\Delta T)(P(n)_{dem}] \tag{2-13}$$

where P_w and P_s are denoted as the power generated by a specific wind turbine and a single solar panel, respectively, provided in Equation 2-12 and Equation 2-13. N_w and N_s are denoted as the number of wind turbines and solar panels used, t is used as the sampling time and ΔT is used as the time interval of samples.

As such, the value of ΔP should be an average value of zero over the same time period, whereas the positive values of Δp indicate the availability of generation by charging batteries. Otherwise the negative values of Δp implies the generation deficiency by discharging batteries. An equation of energy versus time ΔW is obtained by integrating with ΔP.

$$\Delta W = W_{gen} - W_{dem} \int \Delta P dt \tag{2-14}$$

The energy curve shown in Equation 2-14 can be used to detect the required storage capacity for solar/wind system. Usually, the battery periodically fluctuates from positive to negative energy peaks. Therefore, the battery should possess a capacity more than the difference between the positive and negative energy peaks.

In order to minimize the value of ΔP, the step above is repeated based on different combinations of solar panels and wind turbines for the purpose of energy balance.

2-6 Energy Storage

The unpredictable characters of intermittent energy sources such as photovoltaics and wind turbines are discussed above, the mismatch between demand and supply exist during the operation. In order to strengthen power networks and maintain load levels, the energy storage system can adapt energy production to energy consumption, viz., the energy is stored when production exceed consumption and the stores are re-used when consumption exceed production[21].

Battery storage is one type of various storage methods commonly used for direct current (DC) electric power networks, but its disadvantage is involved in its expenditure regarding high maintenance and limited lifespans. With advances of novel technologies, the liquid metal (NaS) battery is currently applied with cheap implementation for large-scale storage, especially used in Japan and United States. Another advantage of this type battery is related to its relatively higher efficiency of charge and discharge (89/92%). But its drawback is also obvious, with the high cost range closer to €350-450/kWh.

Hence, the abundant energy can be stored into another form and transformed back if needed. In order to achieve the electricity storage effectively, some electrical devices are employed to convert electric power from one to another form. Since the solar panels and batteries are operated on DC, DC-DC converters are used for regulate voltage. As the wind turbines is operated on alternating current (AC), AC-DC converters are required. In addition, the loads are operated on AC, inverters are broadly used to supply AC power from batteries. The abovementioned topology is illustrated in Figure 2-14. Due that the bespoke converts cause energy losses, this led more losses than the battery cycle only. Assumed that the efficiency of each converter was 96%, the overall efficiency of the conversion procedure is approximately 75%.

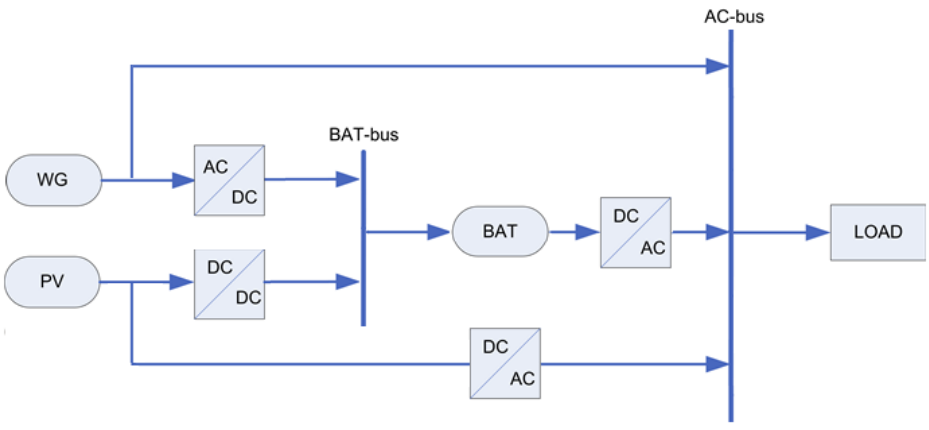

Figure 2-14: Energy storage system topology

The distributed battery storage system is attached to the solar panel and wind turbine. It can directly be seen that the energy redundancy produced by the supply device will flow to the battery and not to the AC-side.

2-7 System Expense

Economic benefit is treated as another critical element to evaluate the solar/wind system. In this section, the electricity cost components including investment and operation costs are analyzed.

The investment cost of the energy supply system is dominated by the costs of the solar panel and wind turbine device, comprising material and installation costs. After consulting several retail price of the real production, the assumed investment cost for all system components is estimated. All solar panel and wind turbine costs are calculated per kW installed peak power, the maximum output under standard test conditions (not the maximum possible output), while the battery costs are calculated per installed kWh.

In this study, the operation cost comprised maintenance and spare parts. The price of each component is assumed to be constant over the years, and considered as per installed kW. Other expenditures such as payback and interest are neglected.

Table 2-2: Assumed investment cost of all system components

Component	Investment	Unit	Maintenance	Unit
Solar panel	2500	€/kW_p	10(0.4%)	€/kW_p per year
Wind turbine	3200	€/kW_p	18.75(0.6%)	€/kW_p per year
Battery	400	€/kWh	4(1%)	€/kWh per year
DC-DC Converter	120	€/kWh	1.2(1%)	€/kW_p per year
DC-AC Inverter	440	€/kWh	4.4(1%)	€/kW_p per year

Therefore the electricity kilowatt-hour (kWh) price containing all cost per year can therefore be calculated by dividing the yearly cost via the amount of kilowatt-hours used during the year.

2-8 Summary

In this chapter, a generic method to achieve the energy balance was described in each individual step. First, the historical weather data was used and the measured data from other country was collected. Then, combined with the relationship between the original data and energy produced, the value of the energy supply could be determined. After that the maximum scale of the different supply device were determined with some restrict. Following

operational strategies were used to execute the algorithm. Finally, the cost of each device were listed, which could be used to calculate the expense of the whole system. In the next chapter, the model of energy demand and supply and study case were provided in details.

Chapter 3

Grid Modeling

3-1 Introduction

In this chapter, the result of the simulation was shown and the used model was created with MATLAB. The model calculated the power difference between supply and demand for every 5 minute intervals during a year. First, the real household data in 2007 and 2008 could be scaled to assume part of the energy demand, combined with the amenity and office part estimated from the ideal data. Then, the 10 year (2001-2010) real measured climate data could be used to show the energy supply. Since there were a large section of solar irradiance data missed in 2007, only the data in 2008 was complete to be used to show the overview of the power flow.

The supply and demand of energy were compared in order to makes sure the demand was always met by the supply. The mismatch between them was stored, shifted and filled by battery. The losses of energy conversion and the storage losses were taken into account when calculating the energy balance. Considering the expense and the space, the capacity of the battery should be limited. If the battery was full, the remaining part of the abundant energy would be dealt with in other ways such as selling to the grid or consuming in local. The amount of energy that flowed into the battery was compared with the amount of total energy consumption, showing the percentage of energy that had to be stored before it could be used.

After all the parameters were determined, the yearly simulation has achieved to make a cost analysis. By changing the supply scale, a cheaper expense could be got and it would be a optimal result.

3-2 Scenario Description

In this project, two urban scenarios were considered. One called Green scenario, which focused on the comfortable living environment and more green plant, so the building height was restricted up to four stories high and 50% open space of the roof were available for solar panel. Another Smart scenario placed extra emphasis on the function of the city, so there were more high buildings could be built in the area. and solar panel installation place was limited to 25% of the roof. The urban plan could be seen in Appendix A, and more detail of the height of the building were listed below.

Table 3-1: Building density

	Green scenario			Smart scenario		
fsi (maximum)	1.9	1.5	1.1	1.9	1.5	1.1
fsi: floor / surface area						
maximum number of layers	4			20		
percentage	80%	50%	30%	20%	15%	10%
other average number of layers	3	2	1.1	4.5	3.55	2.7
percentage	20%	50%	70%	80%	85%	90%
total average number of layers	3.8	3	2.2	7.6	6	4.4

From second row of the table, it could be seed that in the fsi range 1.5 to 1.9, 80% of the building had 4 layers, and the remaining 20% of the building had an average 3 layers, so the average layer on this range of building were 3.8 layers. Other rows were in the same situation, which means all the building were divided into 3 categories with different fsi.

In Green scenario, more solar panel could be built, but the small scale wind turbines were located on a lower height, while in the Smart scenario, less solar panel could be installed, but more wind power could be produced.

3-3 Energy Demand

The electrical load profile of Stadshavens included the house, office and amenity loads. Currently, the specific area contained two blocks: viz., one occupied approximately 122.139 m^2, with averagely 3.5 levels, for living; the other contained 11000 m^2 offices, 11000 m^2 companies and 37000 m^2 amenities.

Up to 2020, 8000 m^2 amenities, 30000 m^2 offices and 74200 m^2 companies will be added to this area. The details of the building type distribution were listed below and the load profile could be known as follow.

Coming to 2030, additional 2930 houses (assumed that a house occupies averagely 125 square meters), 37000 m^2 amenities, 80500 m^2 offices and 118500 m^2 companies will be planned for this area.

In the final 2040, 2040 houses, 33800 m^2 amenities and 12500 m^2 offices will be added to this area. The details of the building type distribution were listed below.

Table 3-2: The building distribution from 2020 to 2040

	2020		2030		2040	
	area	fsi	area	fsi	area	fsi
House (won)	n/a	n/a	140*125	0.6	320*125	1.3
			690*120	1.2	150*120	1.5
			380*125	0.9	700*125	1.75
			660*125	1.9	220*125	1.3
			380*125	1.5	350*125	1.3
			380*125	1.6	300*125	1.4
			300*125	1.2		
Amenity (sv)	8000	1.3	13000	0.9	8800	1.3
			4000	1.3	10000	1.5
			20000	1.9	10000	1.3
					5000	1.75
Office (kant)	1000	1.75	20000	1.3	12500	1.5
	2000	1.3	5000	1.75		
			4000	1.4		
			5000	1.3		
			6000	0.9		
			30000	1.9		
			3000	1.6		
			7500	1.2		
Company (bedr)	320	1.3	27500	1.3	n/a	n/a
	40000	1.3	21000	0.6		
	15000	1.75	5000	1.4		
	6000	1.4	5500	1.3		
	10000	1.3	49000	1.9		
			3000	1.5		
			7500	1.2		

Since the building distribution had been listed, combing with the pu load curve which described in the previous chapter, the ideal daily load profile can be shown as follows.

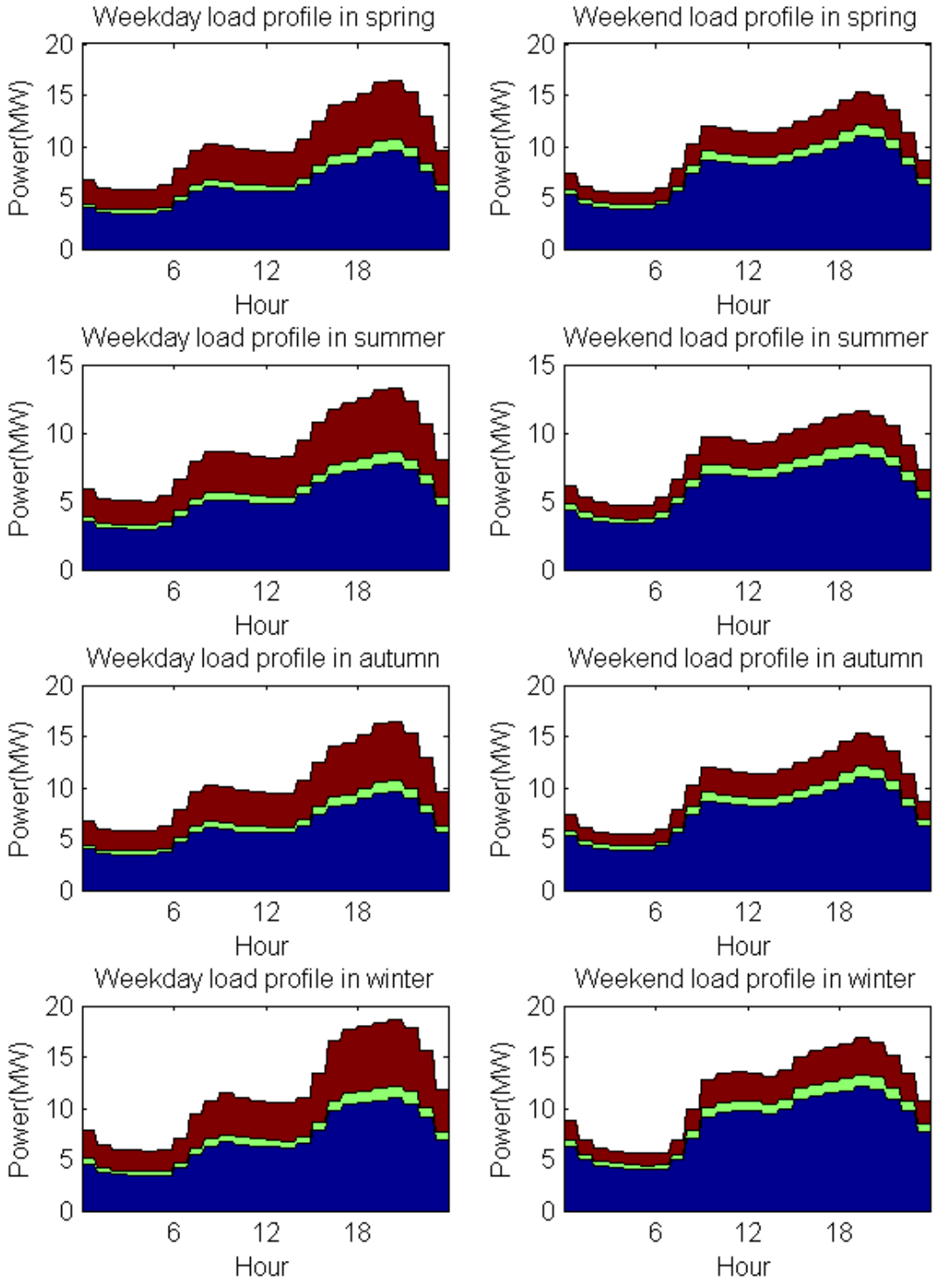

Figure 3-1: Daily load profile in 2040

Based on the ideal average daily load curve, the yearly load variation could be estimated. The yearly amenity and office load curve were built based on the ideal daily load curve. Since the daily curve was not the same in the real case, and to avoid a sudden step between the season, some adjustment was made to produce a gradual change amenity and office yearly load curve. Then, the household load curve was built by amplifying the measured yearly curve to make the sum of it equal to the sum of ideal yearly house load curve. Thus the yearly total load profile could be demonstrated as follows.

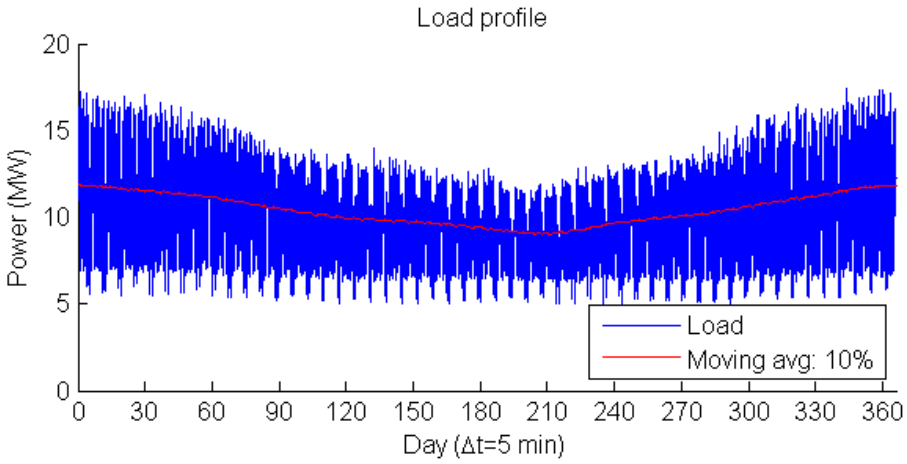

Figure 3-2: Load profile in 2040

From the figure above, the yearly variation of energy demand was shown clearly and its value was also calculated and listed below.

Table 3-3: Energy Demand (MWh) in 2040

	Spring	Summer	Autumn	Winter	Sum
House	13,784	12,224	13,998	16,341	56,347
Amenity	1,587.7	1,471.5	1,570	1,605.8	6,235
Office	7,318	6,898	7,280	7,437	28,933

3-4 Energy Supply

In order to make an energy balance, the yearly energy supply also should be provided. The solar and wind power potential were both described before. In this section, the energy production of solar panel and wind turbine in both scenario were demonstrated in details.

3-4-1 Solar Panel Production

As described before, the solar irradiance corresponded linearly to the solar power. From the yearly solar irradiance curve which shown in the previous chapter, the solar power could be calculated based on it.

In this study, two scenarios were introduced to determine the solar panels for totally-available areas. As indicated in the urban scenario description, for Green scenario, it was assumed that 50% of the building roof areas were available for solar panels, from Figure 2-7, under the GCR 50% the mismatch was 6%. Whilst in the Smart scenario, only 25% were available, the mismatch reduced to 0.15%. The efficiency of solar panel was assumed to be 30% in the year of 2040. Based on this notion, the solar panel will produce $192,262\ MWh$ via Green scenario and $100,733\ MWh$ via Smart scenario in 2040. The calculation results in both scenario were shown below.

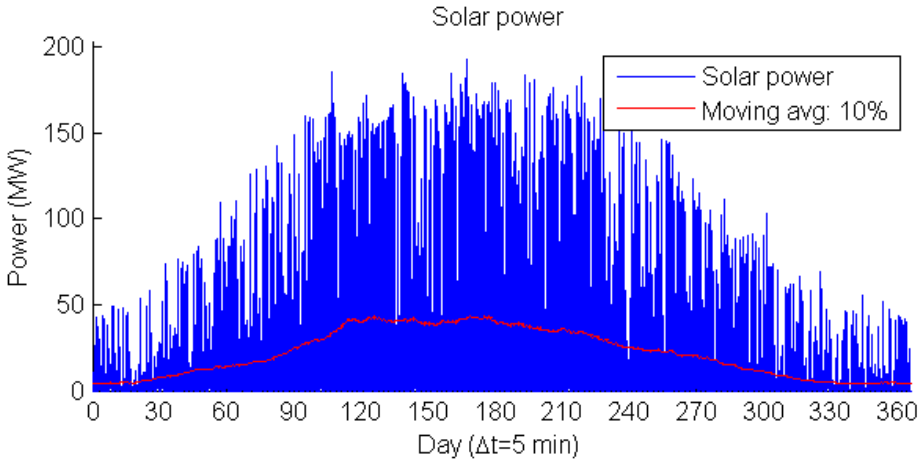

Figure 3-3: Solar power in 2040, Green scenario

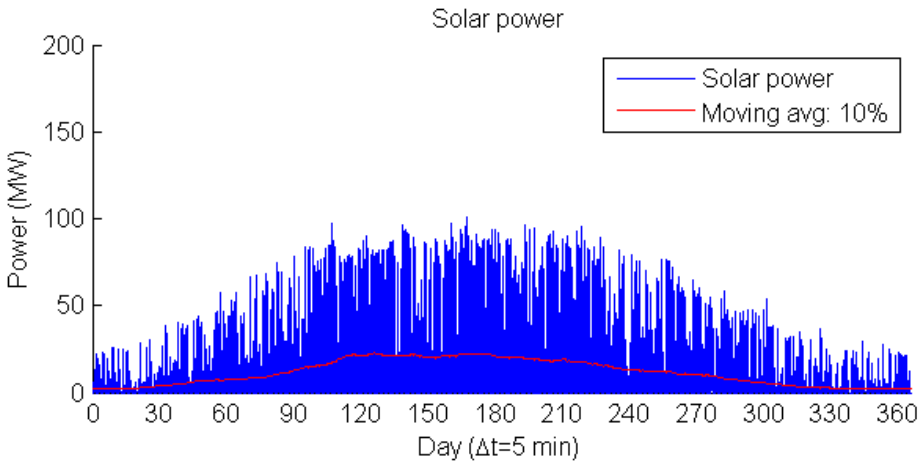

Figure 3-4: Solar power in 2040, Smart scenario

It was common that the solar power were lower in the beginning of the year, and then it increased to the peak in summer, and finally it decreased to the bottom in the winter.

The ideal average daily solar irradiance distribution in four-seasonal days was also be shown in Figure 3-5 and it could be used to reveal the daily solar power. However, it should be noted that this was only a simplified assumption. In the real cases, it was never the same amongst everyday, which would be shown in Appendix B.

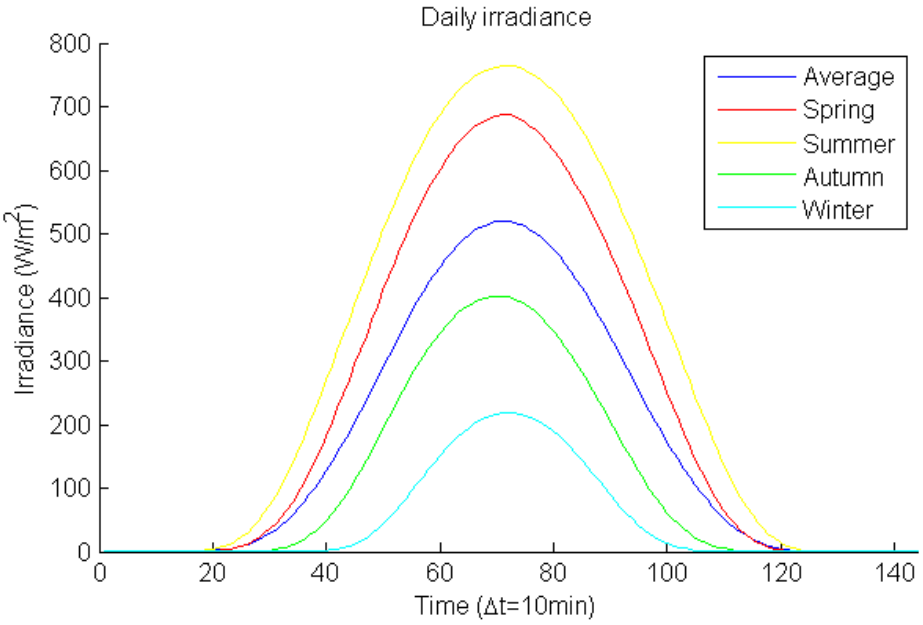

Figure 3-5: Smoothed seasonal daily irradiance

3-4-2 Wind Turbine Production

For the wind power, as discussed in the previous chapter, two types of the wind turbine were installed in this area, one was the large-scale wind turbine built on the ground along the shore, with an axle height of 37 m and a rotor diameter of 34 m. The number of the large wind turbines (24) was the same in both scenario, and its power variation was shown as follows.

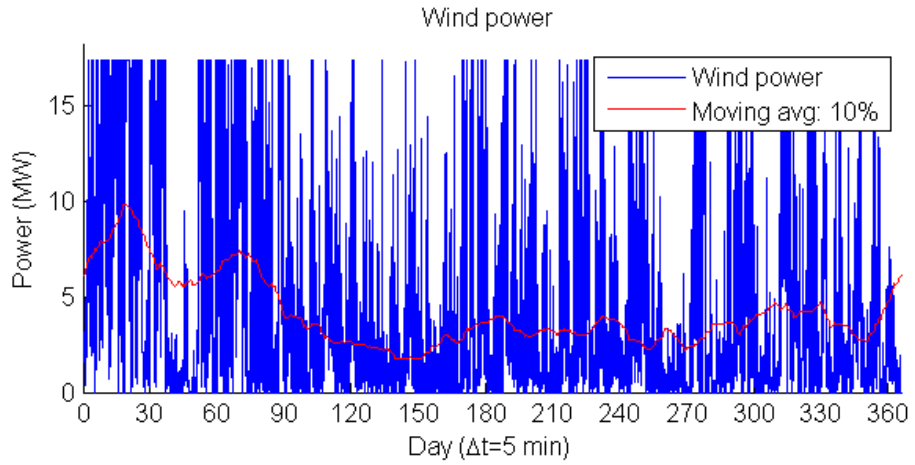

Figure 3-6: Wind power generated by large scale wind turbines in 2040

The other was the small-scale vertical axis wind turbine built on the roof, with the mounting height of 5.5 m and a rotor diameter of 3 m. The average storey was assumed as 3 m. Considering the different building height in the two scenarios, and its number and distribution were all difference.

For Green scenario, the building is divided into three parts with the different fsi, which was show in Table 3-1. The number of the small wind turbine installed on the different storeies of the building (2.2, 3 and 3.8) was 351, 438 and 209. So the power variation generated by these small wind turbine was shown as follows.

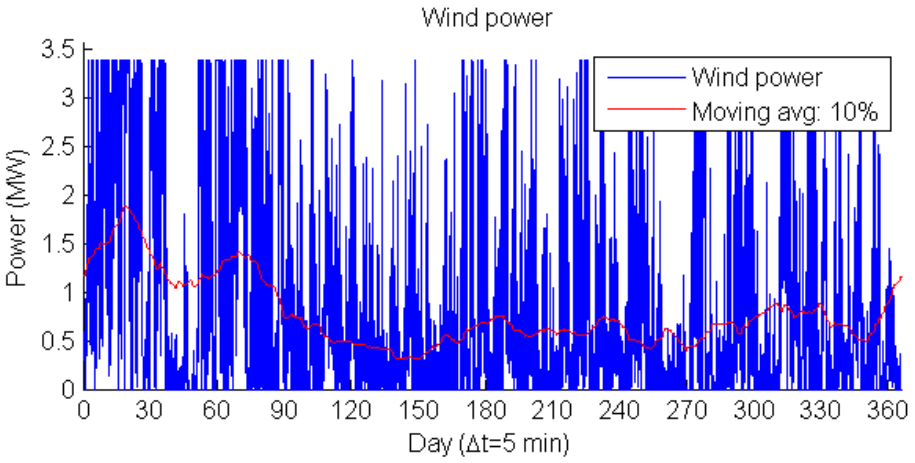

Figure 3-7: Wind power generated by small scale wind turbines in 2040, Green scenario

For Smart scenario, the number of the small wind turbine installed on the different storeies of the building (4.4, 6 and 7.6) was 528, 668 and 314. So the power variation generated by these small wind turbine was shown as follows.

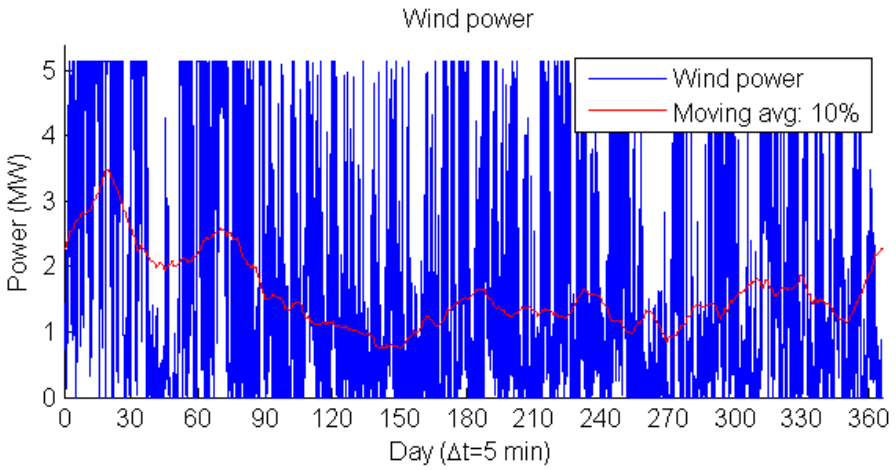

Figure 3-8: Wind power generated by small scale wind turbines in 2040, Smart scenario

Combing the three previous wind power curve, it was clearly that there was significantly larger fluctuations in the whole year, then the average daily wind speed in different season was also presented in Figure 3-9.

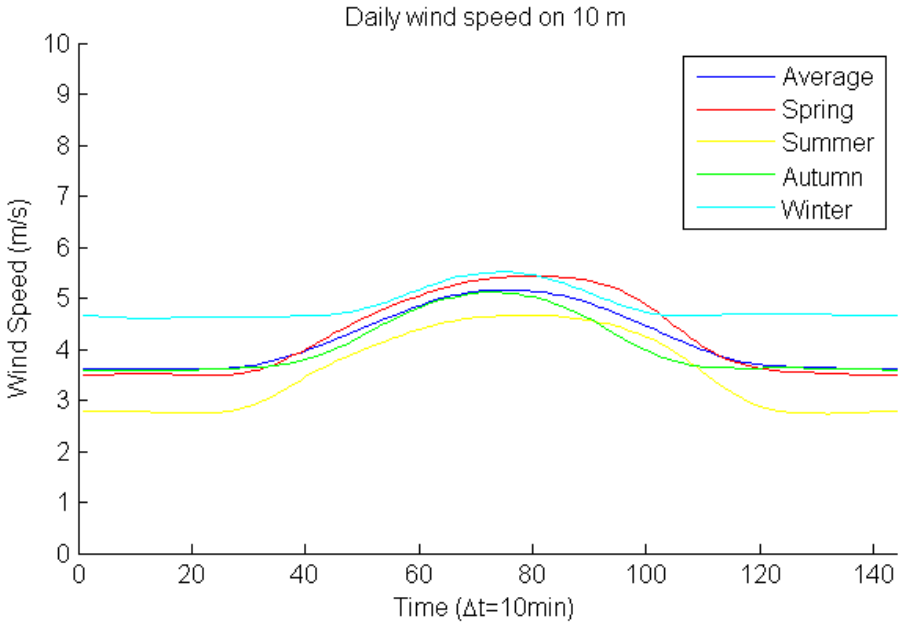

Figure 3-9: Smoothed seasonal wind speed

It should be noted that it was also a simplified approximation. Unlike the solar irradiance had a predictable curve which followed the movement of the sun. The real wind speed was highly variable and different among every single day, which would also be discussed in Appendix B. Nevertheless, this ideal daily wind speed figure could be used to construct the model and deliver a better understanding of the daily energy balance among seasons.

3-5 Power Flow

The previous sections demonstrated yearly variations in demand and supply. In the whole system, the wind turbines directly connected to the load, while the solar panels connected to the load through the solar inverter with 96% efficiency. This section analysis the energy balance for the whole grid in Green scenarios as a sample. It showed how much energy needs to be stored and how much storage is shifted to use.

In 2040, the maximum total yield energy will be $235,604\ MWh$, including $459,202\ m^2$ solar panel ($192,262\ MWh$), 998 small-scale wind turbines ($6,871\ MWh$) and 24 large scale wind turbines ($36,472\ MWh$). and the total energy demand will be $91,514\ MWh$. The percentage of each parts were shown in Figure 3-10 below.

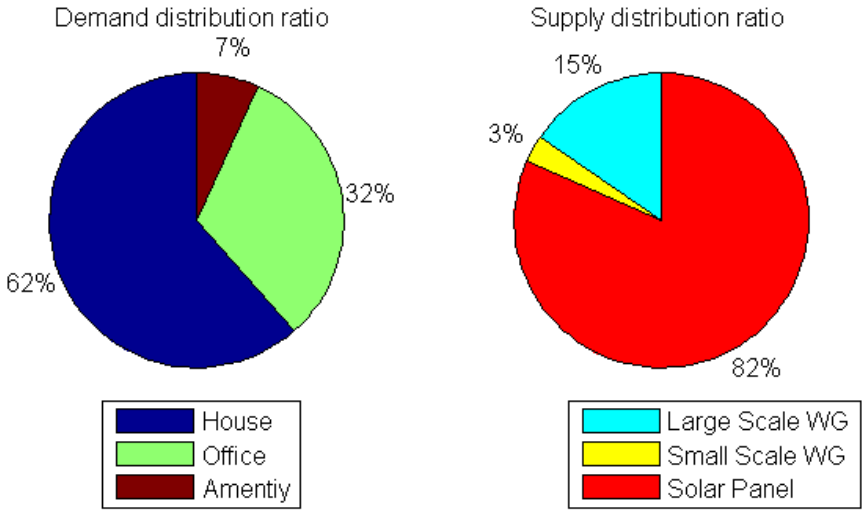

Figure 3-10: Energy distribution in 2040, Green scenario

By using the maximum amount of energy producing, the load demand was matched. Then, the seasonal matching result in 2040 was shown in Figure 3-11.

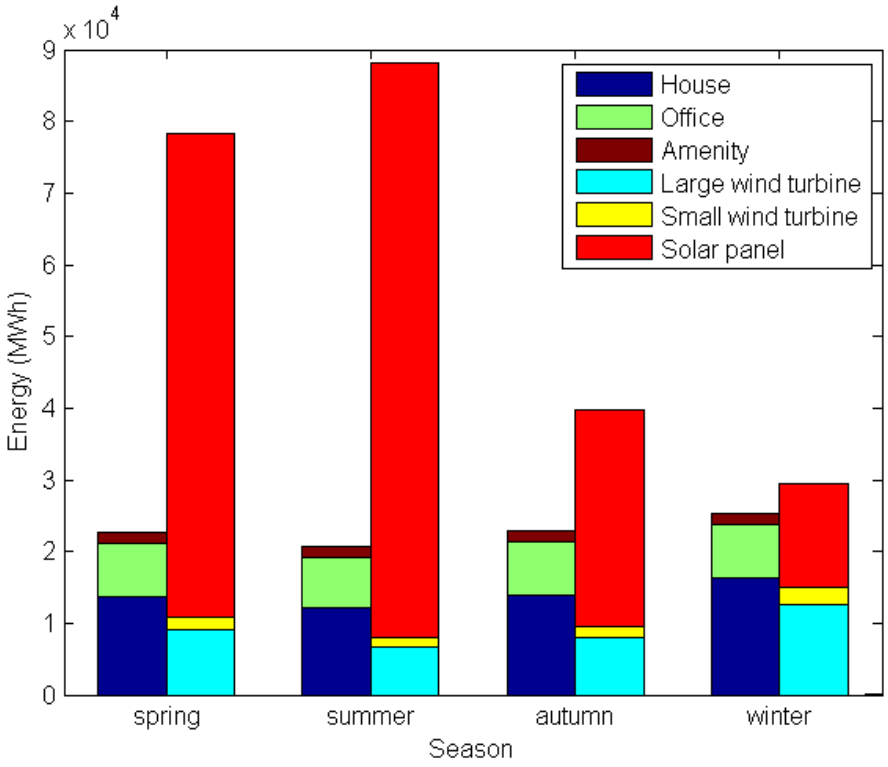

Figure 3-11: Energy balance between demand and supply in 2040, Green scenario

Then, the value of each block was list below in detail.

Table 3-4: Energy balance between demand and supply in 2040, Green scenario

	Supply (MWh)			Demand (MWh)		
	PV	WG (L)	WG (S)	House	Office	Amenity
Spring	67,373	9,127	1,724	13,784	7,318	1,588
Summer	80,073	6,752	1,259	12,224	6,898	1,472
Autumn	30,312	8,022	1,501	13,998	7,280	1,570
Winter	14,503	12,570	2,387	16,341	7,437	1,606

By considering all seasons, the maximum energy supply could sufficiently match the energy demand in the aggregate, even though the difference between demand and supply were all difference. Considering the power variation of demand and supply which described before, it was possible that some power mismatch would take place in some time. So the yearly power flow was simulated in detail. It was critical to determine the storage system.

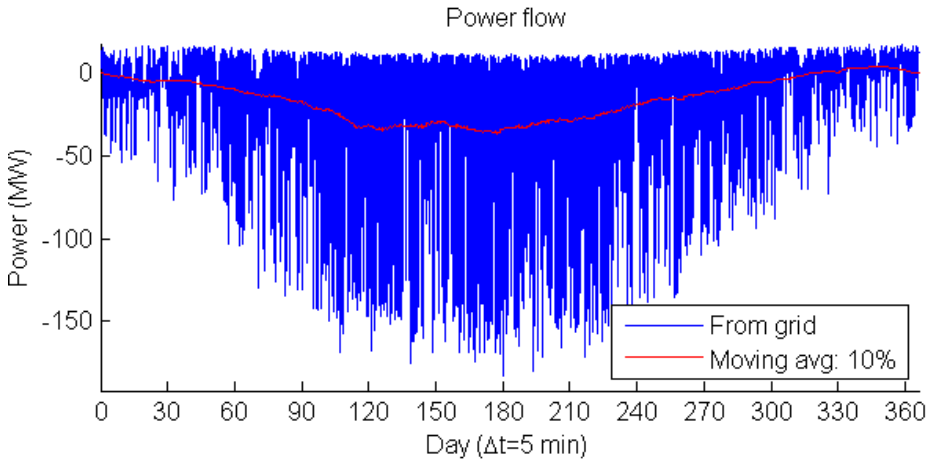

Figure 3-12: Power flow of the area in 2040, Green Scenario

From the blue line in Figure 3-12, it was clear that there were lots of real-time mismatch by comparing the energy demand and supply, so a battery device was needed to store and shift the supply energy surplus. From the red moving average power flow line, it could be reveal that in the last two months of the year, the energy supply could not meet the energy demand, which also could be shown in Figure 3-11.

From Figure 3-12, the negative value was the supply energy surplus ($169,819\ MWh$ in total) which could be stored into the battery, with 89% charging efficiency, and 92% (discharging efficiency) of the battery energy would be used to fill the energy shortage through a DC/AC converter (96% efficiency) to the load in the later time. With the unlimited capacity of the battery, the result of the battery round trip was shown as follows.

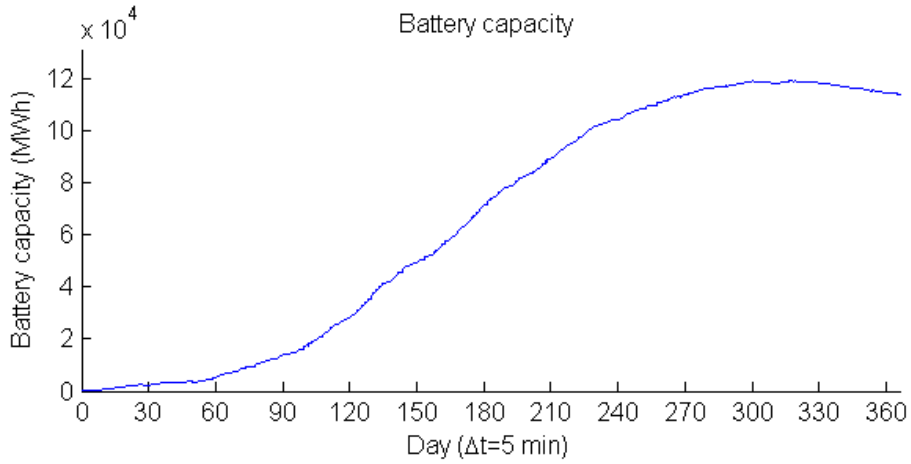

Figure 3-13: Battery charging/discharging situation

From Figure 3-13, with the unlimited capacity of the battery, there were 113, 700 MWh energy accumulated in the battery at the end of the year. These amounts of the energy would never participated in the battery round trip. It was easy to assumed that if there was only one used battery, it was better to dump the energy and produce it again when required. If using such large battery, the battery was in the charge state for a long time, which meant it was an uneconomic solution to store these parts, because large capacity of the battery would cost lots of money and space.

Since the battery device was a critical component in energy balance, the required battery capacity should be known. A suitable required battery capacity was determined by many variables in the system such as the cost of the battery (€/kWh) and maximum charge power.

The maximum charge power was an element which could influence the suitable required battery capacity. From Figure 3-12, the maximum charge power was approximately 180 MW. Choosing a larger charge power, all the energy surplus could be stored. By reducing the charge power, much energy which would not flow into the battery, which caused some energy loss. The relationship between the charge power and the energy loss under these condition was shown as follows.

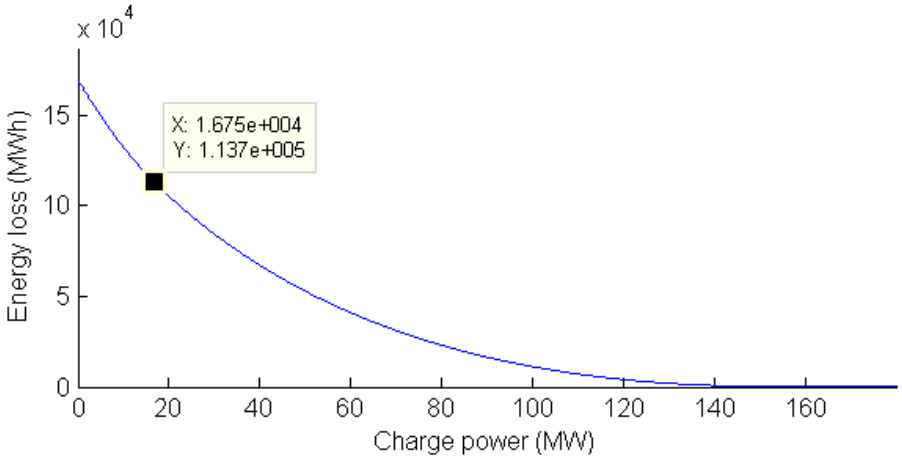

Figure 3-14: Energy loss vs charge power

From Figure 3-14, it shown that 113, 700 MWh energy loss represented that the charge power was 17 MW, which meant choosing a larger charge power was not worthwhile. The charge rate (C rate) also influenced the required battery capacity, in this project, the maximum charge rate was recommended slower than C/10.

Therefore, the battery capacity was assumed as 170 MWh at first. The yearly charging/discharging round trip was simulated and shown as follows.

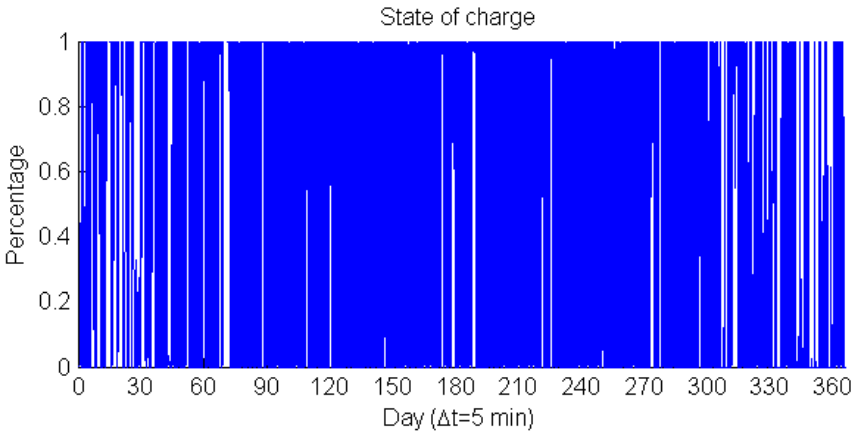

Figure 3-15: 170 MWh battery state of charge, Green scenario

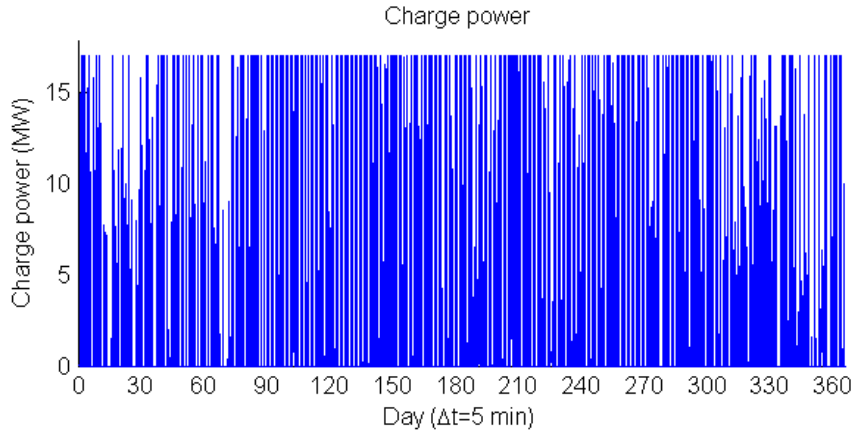

Figure 3-16: 170 MWh battery charge power, Green scenario

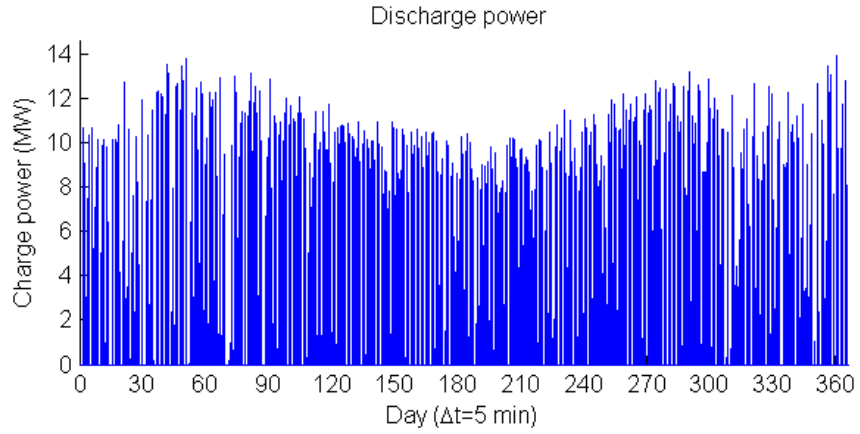

Figure 3-17: 170 MWh battery discharge power, Green scenario

It was clear that the battery round trip frequency was almost once a day. With the lifetime of 3,000 cycles (at 90% DOD - depth of discharge), the battery could be used in 8 years. Then, the value of the charge/discharge part situation were also shown.

From Figure 3-16 and Figure 3-17, with the total 170 MWh battery capacity, totally $5,689$ MWh energy charge in the battery and $4,472$ MWh energy discharge from the battery could compensate the energy shortage. Then the result of the power flow which added the battery was shown as follows.

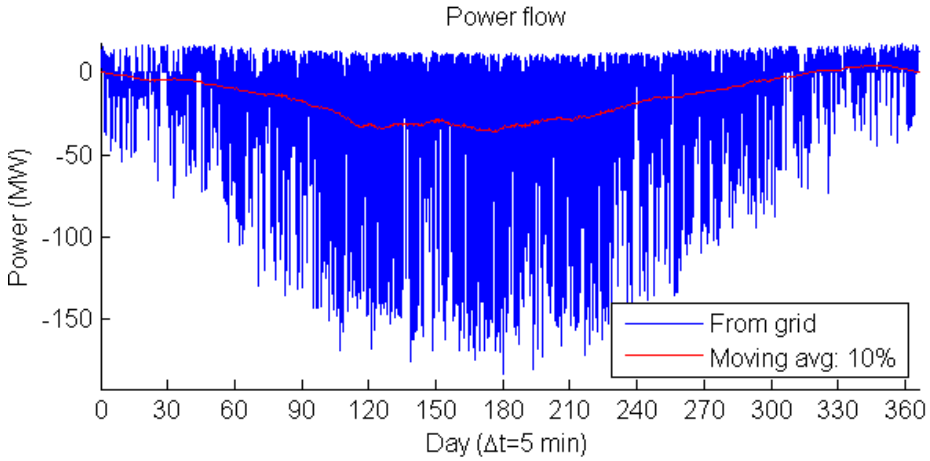

Figure 3-18: Power flow after charging/discharging

From Figure 3-18, there were still lots of superfluous energy in the whole year, and the energy shortage still existed after adding the battery storage device. From Figure 3-13, it could be concluded that the approximate $120,000$ MWh of the battery capacity was able to fully meet the energy compensation, and this larger capacity was uneconomic and also unrealistic, Since it would cost lots of expense and occupied lots of area. Thus, expanding the battery capacity was not recommended. In such situation, these superfluous energy could not be used in the area and some extra energy should be entered from outside.

3-6 Cost Analysis

A cheaper electricity price was an important indicator to make the energy balance. The price containing all cost could therefore be calculated by dividing the yearly cost via the amount of kilowatt-hours used during the year. In this section, the electricity cost components including investment, operation and other costs were analyzed to determine the size of the battery.

First, the individual investment cost of the energy supply system which described in Section 2-7. Specifically for this study, the peak power of the solar panel per square meter and the DC-AC inverter were set as 0.4 kW, the peak power of the individual large scale wind turbine

was set as 750 kW, and the peak power of the individual small scale wind turbine was set as 3.4 kW. In Green scenario, the solar panels covered 459, 202 m^2, and the number of large and small scale large wind turbines was 24 and 998, respectively. The battery capacity was 170 MWh. and the total peak power of the DC-DC converter was 17 MWh. Thereby the total expenditure was € 696, 879, 792.

Then, the cost of the energy exchange were calculated, referring the policy of electricity delivery back to the grid, the cases of two companies were shown as follows.

- Nuon

  When the client provided up to 5, 000 kWh a year ago and the difference between delivery by Nuon and the client return delivery to Nuon is negative (= the client supply more electricity back than Nuon produces). The client's restitution is fully delivered back by Nuon. When the client provided more than 5, 000 kWh a year ago. The client's maximum of 5, 000 kWh restitution is fully delivered back by Nuon. The client will not receive compensation for the restitution equal to the price pay for delivery, including energy tax and VAT. For the part of the client's restitution that exceeds the supply by Nuon, The client will receive a fee for return of € 0.0588/kWh.

- Essent

  The maximum redelivery energy is 5, 000 kWh a year, For the the client provided the first 3, 000 kWh, a total fee, including energy, taxes, transportation and delivery is roughly equivalent to € 0.2149/kWh. For the next 3001 to 5000 kWh, the customer will receive a fee equivalent to the delivery rate € 0.086/kWh, then deducting the tariffs € 0.039/kWh. On the other hand, the electricity from the grid need to be paid separately, € 0.2275/kWh including energy tax and VAT, for the first 10, 000 kWh.

Since the meter was installed at the client side, the energy transmission loss were not needed to be considered. Specifically for this study, after using the battery to store and shift the energy, 164, 130 MWh were still redundancy, which could be return to the grid. 28, 947 MWh energy should be bought from the grid. Considering the individual maximum electricity the grid could delivery back was 5 MWh, the total energy could be divided into 32,826 parts. For Nuon case, the difference between delivery by grid and return delivery to grid is negative (135, 183 MWh), with the price € 0.0588/kWh, the total compensation was € 7, 948, 760. While for the Essent case, there were no compensation in total, which meant the Nuon case was more beneficial. As a result, the energy supply and demand were both divided into three part, which shown as follows.

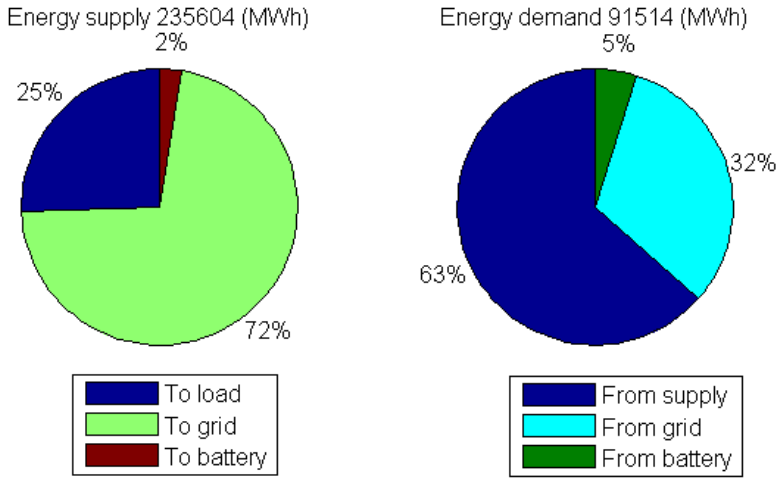

Figure 3-19: Energy distribution, Green scenario

Based on the energy distribution, the component of the total yearly cost were list below.

- Investment cost, dividing into 20 years (lifetime of the supply device), 8 years (lifetime of the battery) and 10 years (lifetime of DC-DC converter and DC-AC inverter).
- Maintenance cost, including solar panel, wind turbine, battery, DC-DC converter and DC-AC inverter.
- The cost from the operation of the battery storage and the price was €0.10/kWh.
- The cost from the energy difference which compensate from the grid, which was €0.0588/kWh.

Hereby, the electricity kilowatt-hour (kWh) price in proposal one was calculated and listed below.

Table 3-5: Cost overview

Cost Fraction	Investment	Maintenance	Total €/year
Solar panel	45,9202,000	1,836,808	
Wind turbine	68,458,240	410,750	
Battery	68,000,000	680,000	
Convert	20,400,000	204,000	
Inverter	80,819,552	808,196	
Storage			568,908
Energy subsidy			8020,333
Electricity Cost	€0.4063/kWh		

3-7 Optimization Analysis

From the cost analysis, it was clear that more supply device could generated more energy, which also brought more investment device cost, and if these energy production could not be used, it would left more energy redundancy and sold to the grid with a low recycling subsidies price. And from the Figure 3-19, such large battery could only store small part of the energy redundancy, but the battery price was quit high.

In order to eliminate these energy mismatch and reduce the electricity price, two proposals were proposed as follows.

1. Proposal 1: Changing the battery capacity.
2. Proposal 2: Changing the energy supply device.

By comparing the result of the two proposals above, the electricity kilowatt-hour (kWh) price could be calculated and used to choose the optimum one.

3-7-1 Proposal one

In the initial analysis, expanding the battery capacity was not recommended, but comparing the cost of the battery and the supply device, it was clear that the battery expense was much high, and it could only store a small portion of the excess energy (approximately 2%).

In this proposal, the battery would first drop to the half of the original capacity and finally removed. the supply device were no change. As a result, the electricity kilowatt-hour (kWh) price with 100 MWh battery and with no battery were calculated and listed below.

Table 3-6: Cost overview with 85 WMh battery

Cost Fraction	Investment	Maintenance	Total €/year
Solar panel	45,9202,000	1,836,808	
Wind turbine	68,458,240	410,750	
Battery	34,000,000	340,000	
Convert	10,200,000	102,000	
Inverter	80,819,552	808,196	
Storage			309,408
Energy subsidy			8020,333
Electricity Cost	€0.3478/kWh		

Table 3-7: Cost overview without battery

Cost Fraction	Investment	Maintenance	Total €/year
Solar panel	45,9202,000	1,836,808	
Wind turbine	68,458,240	410,750	
Inverter	80,819,552	808,196	
Energy subsidy			8020,332
Electricity Cost	€0.3224/kWh		

From the two table above, it could be revealed that the battery storage system was not necessary, without the battery device, the electricity price would be substantially reduced.

3-7-2 Proposal two

From Figure 3-11, it could be found in spring and summer the energy supply was more than the energy demand, especially for the solar power. The subsidy of energy sold to the grid was quit low, this proposal was to reduce the supply device, especially the solar panel.

In Green scenario, the small scale wind turbine and solar panel occupied the same area on the roof of the building, but the energy produced by the small wind turbines was less than the solar panels, even in autumn and winter. In thus situation, the small wind turbines were first removed, following the solar panels were reduced.

By removing the small scale wind turbine, the energy distribution was updated.

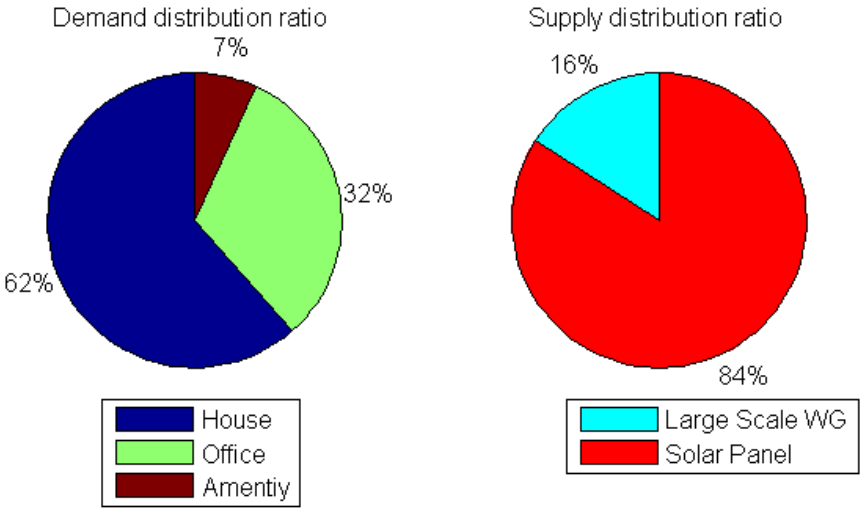

Figure 3-20: Energy distribution in 2040, Green scenario, Proposal 2-1

The percentage of each parts were changed and shown in Figure 3-20 above. The total yield energy will be $228,734\ MWh$, including 459202 m^2 solar panel ($192,262\ MWh$) and 24 large scale wind turbines ($36,472\ MWh$). and the total energy demand still would be $91,514\ MWh$. Then, the seasonal matching result in 2040 was also shown in Figure 3-21.

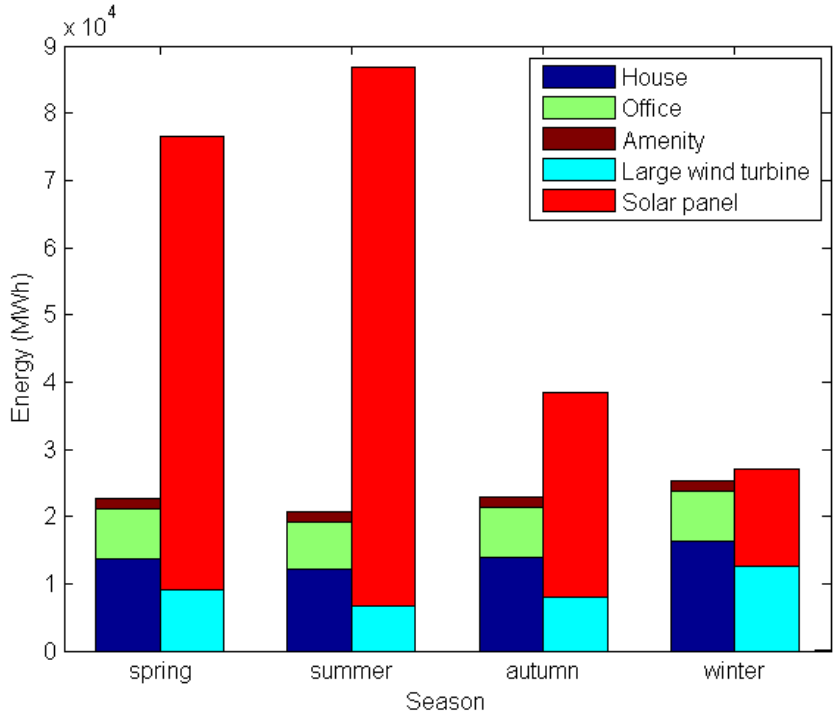

Figure 3-21: Energy balance between demand and supply in 2040, Green scenario, Proposal 2-1

By considering all seasons, the maximum energy supply could sufficiently match the energy demand in the aggregate, even though there appeared energy shortage in autumn and winter. The yearly power flow was also simulated in detail.

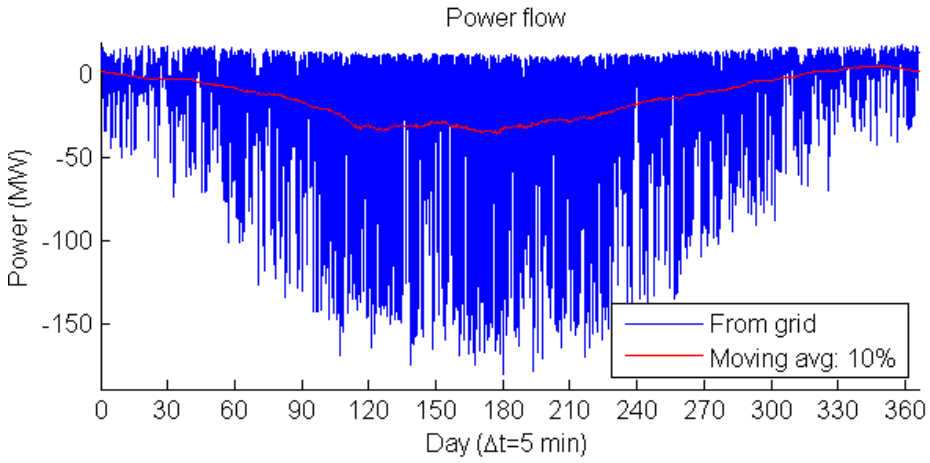

Figure 3-22: Power flow of the area in 2040, Green Scenario, Proposal 2-1

From Figure 3-22, 164, 333 MWh superfluous energy would not be directly used and sold to the grid. In order to meet the energy balance, 34, 804 MWh could bought back from the grid, which meant the difference 129, 529 MWh could get subsidy. As a result, the energy distribution were shown as follows.

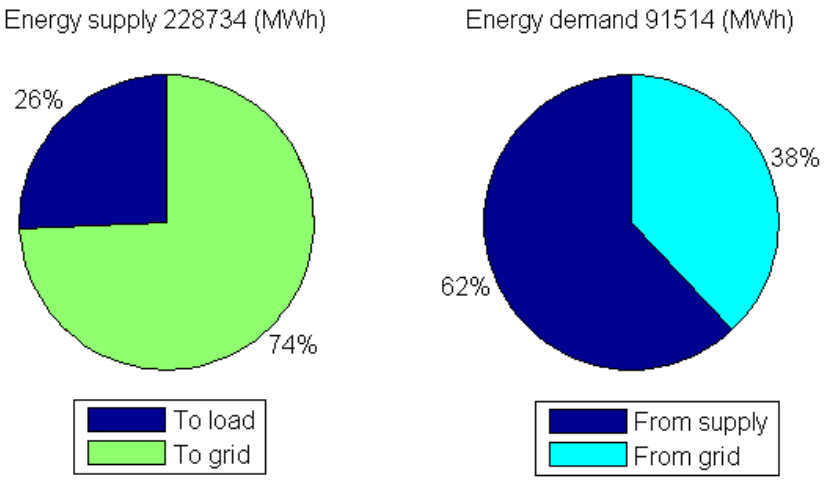

Figure 3-23: Energy distribution, Green Scenario, proposal 2-1

Thus the electricity kilowatt-hour (kWh) price in proposal two was calculated and listed below.

Table 3-8: Cost overview without small wind turbine

Cost Fraction	Investment	Maintenance	Total €/year
Solar panel	45,9202,000	1,836,808	
Wind turbine	57,600,000	345,600	
Inverter	80,819,552	808,196	
Energy subsidy			7,616,325
Electricity Cost	€0.3201/kWh		

It was clear that removing the small scale wind turbine, energy used more efficiently. and some open area were available. Since there were still lots of energy redundancy in spring and summer, it was possible to reduce some solar panels. Based on these strategy, an advanced proposal was emerged, which reduced 50% the solar panels. The percentage of each parts were changed and shown in Figure 3-24 below.

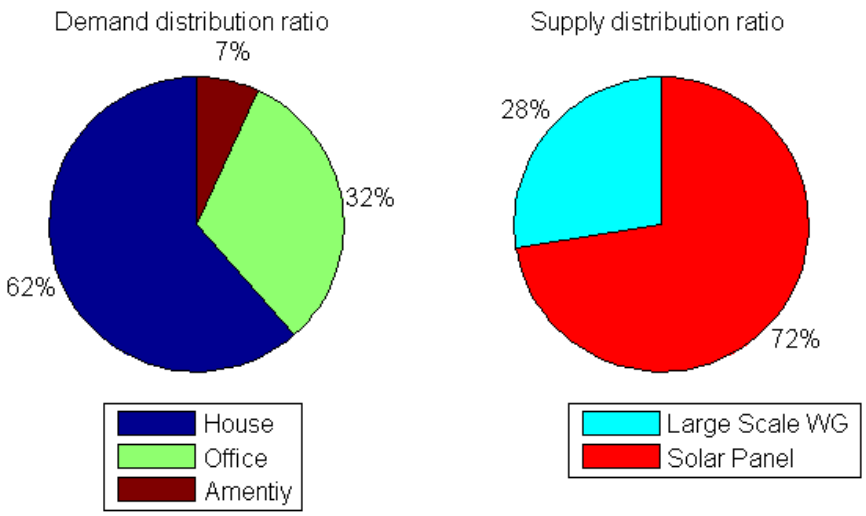

Figure 3-24: Energy distribution in 2040, Green scenario, Proposal 2-2

The total yield energy would be $132,603\ MWh$, including $229,601\ m^2$ solar panel ($96,131\ MWh$) and 24 large scale wind turbines ($36,472\ MWh$). and the total energy demand would be $91,514\ MWh$. Then, the seasonal matching result in 2040 was also shown in Figure 3-25, and the yearly power flow was also simulated in detail.

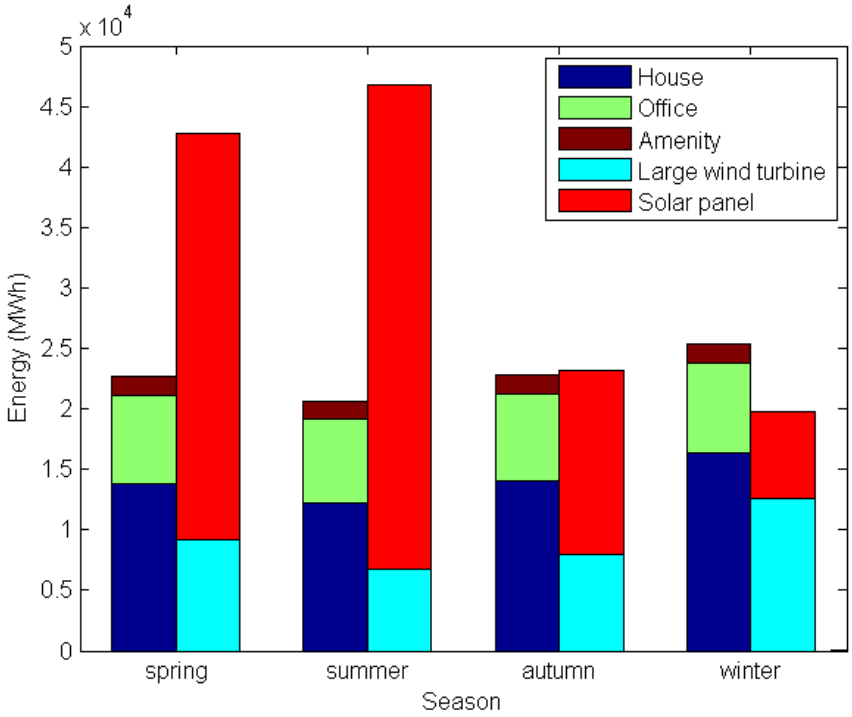

Figure 3-25: Energy balance between demand and supply in 2040, Green scenario, Proposal 2-2

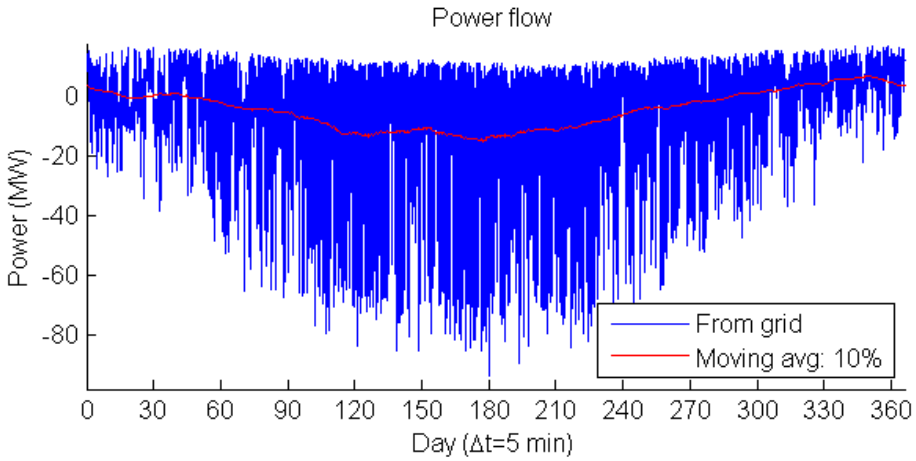

Figure 3-26: Power flow of the area in 2040, Green Scenario, Proposal 2-2

From Figure 3-26, 74,808 MWh energy surplus would not be directly used and sold to the grid. In order to meet the energy balance, 37,564 MWh could bought back from the grid, which meant the difference 37,244 MWh could get subsidy. As a result, the energy distribution were shown as follows.

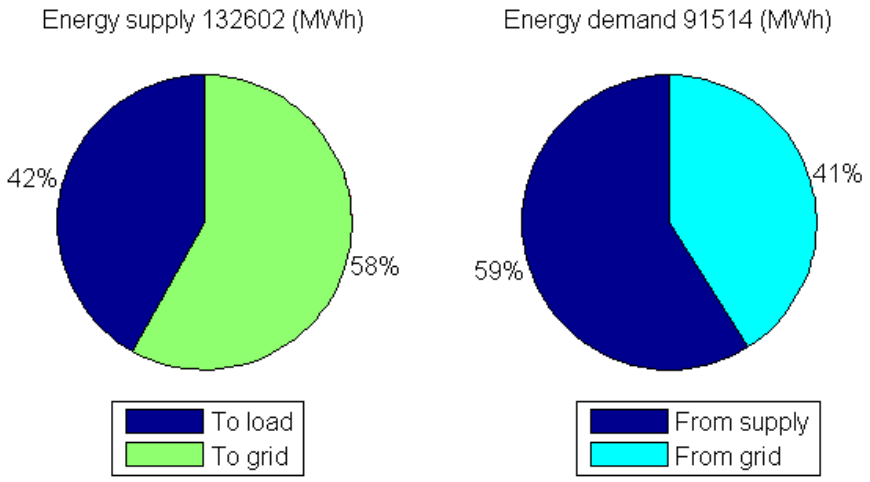

Figure 3-27: Energy distribution, Green Scenario, proposal 2-2

Thus the electricity kilowatt-hour (kWh) price in proposal two was calculated and listed below.

Table 3-9: Cost overview with 50% original solar panels

Cost Fraction	Investment	Maintenance	Total €/year
Solar panel	229,601,000	918,404	
Wind turbine	57,600,000	345,600	
Inverter	40,409,776	404,098	
Energy subsidy			2,189,913
Electricity Cost	€0.1954/kWh		

The proposal two shown that choosing the suitable solar panel area could get a optimum lower price of the electricity. It verified that reducing the difference between demand and supply could drop the electricity price and using the energy efficiently.

Following, the relationship between the percentage of the energy via grid and the ratio of the energy supply and demand were shown as follows.

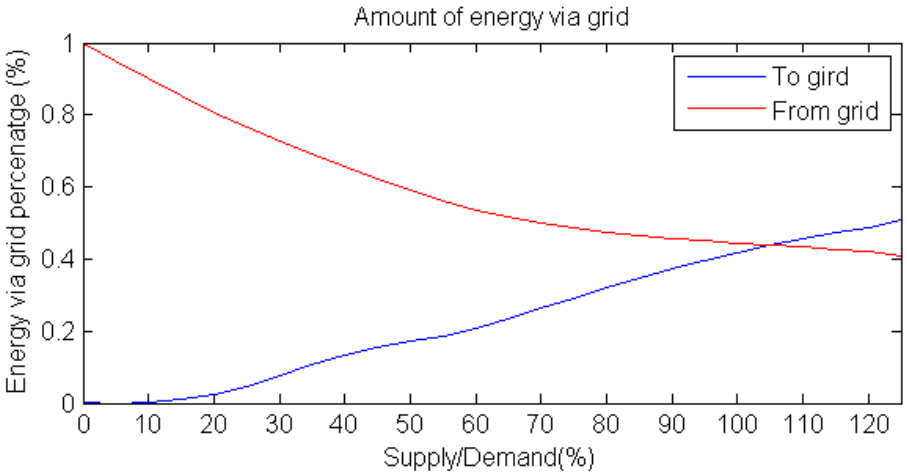

Figure 3-28: Amount of energy via grid

Since the energy produced from solar panel connected to the load through a inverter and would cause some conversion loss, the total amount of energy supply should be larger than the energy demand. Only when the energy transfered to the grid more than the energy returned from the grid, it could not pay extra money to buy the electricity with a high price. From the Figure 3-28, on the left side of the intersection, the energy supply is less than the energy demand, which meant extra energy should be bought from the grid with a high price, while on the right side of the intersection, the energy supply is more than the energy demand, which meant the energy redundancy should be sold to the grid with a low price. The optimum electricity price would located on the intersection, which meant the supply device could be reduced. Based on these proposal, the optimum result of both scenario could be determined and shown in the next section.

3-8 Scenario Result

The previous sections demonstrated yearly variations in demand and supply. Based on the power flow, the cost were analyzed. By comparing the two improved proposals, the influential parameter to the electricity price would be shown, and it revealed that the battery was not a necessary part in the process of the energy balance. In this section, the optimum supply device scale would determined, and a cheaper electricity price could be got in two scenarios.

3-8-1 Green Scenario

The maximum energy supply vs energy demand were shown in Section 3-5. Through the iterative algorithm in detail, the small wind turbines on the roof of building would be removed. The total yield energy would be $94,559\ MWh$, including $130,413\ m^2$ (14.2% of the roof area with no mismatch) solar panels ($58,088\ MWh$) and 24 large scale wind turbines ($36,472\ MWh$). The total energy demand would be $91,514\ MWh$. By considering all seasons, the maximum energy supply could sufficiently match the energy demand in the aggregate, even though there appeared energy shortage in autumn and winter. The value of each part of the seasonal demand and supply were shown and list below in detail.

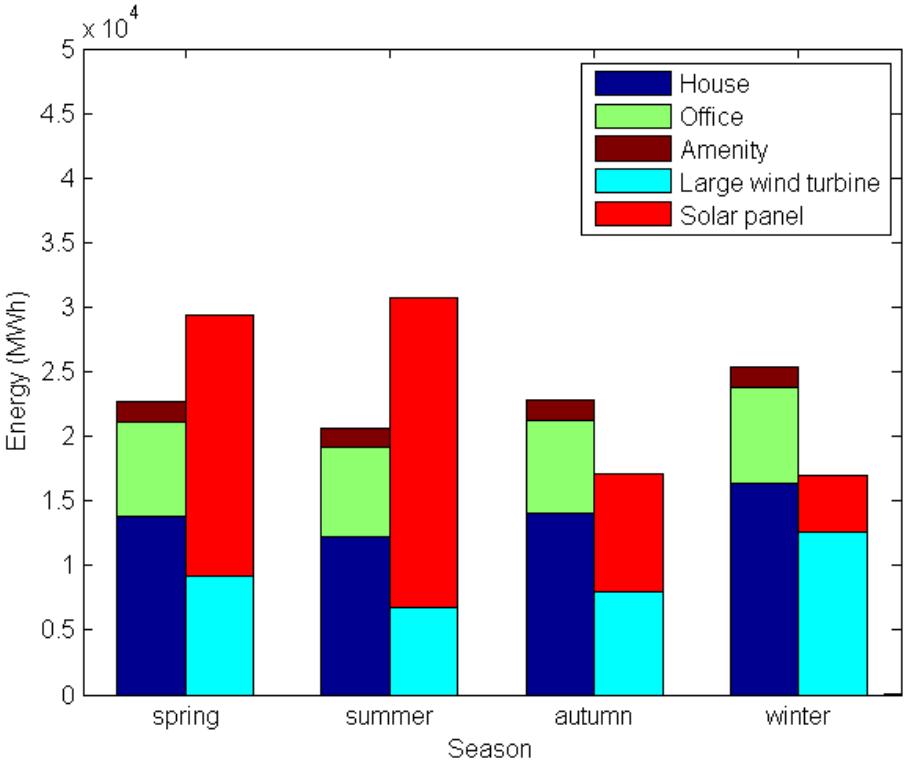

Figure 3-29: Energy balance between demand and supply in 2040, Green scenario

Table 3-10: Energy balance between demand and supply in 2040, Green scenario

	Supply (MWh)		Demand (MWh)		
	PV	WG	House	Office	Amenity
Spring	20,355	9,127	13,784	7,318	1,588
Summer	24,192	6,752	12,224	6,898	1,472
Autumn	9,158	8,022	13,998	7,280	1,570
Winter	4,382	12,570	16,341	7,437	1,606

The percentage of each parts were changed and shown in Figure 3-30 below.

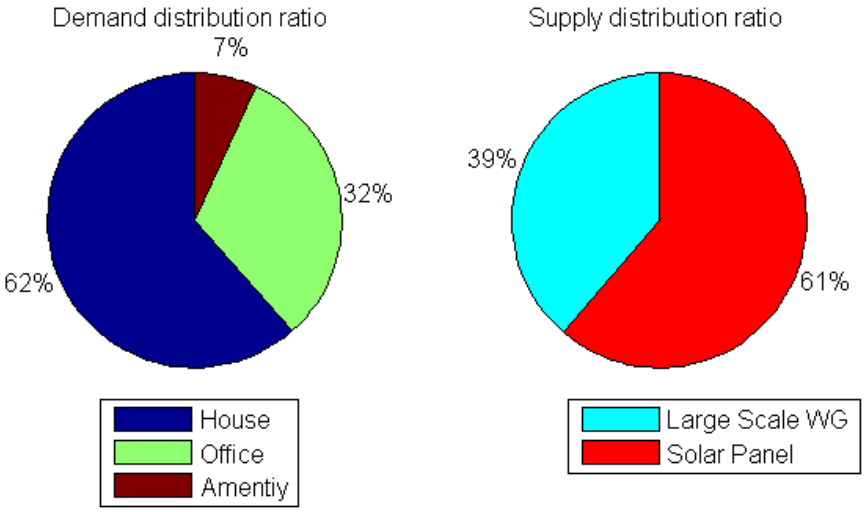

Figure 3-30: Energy distribution in 2040, Green scenario

The yearly power flow was also simulated in detail.

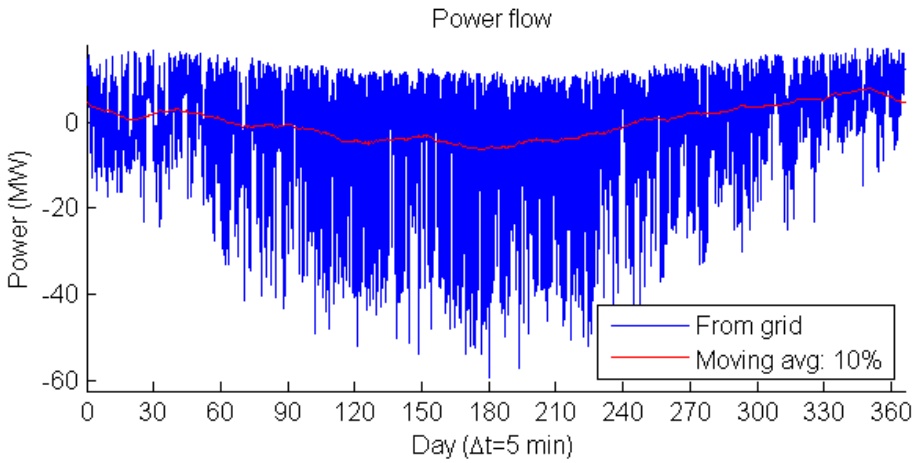

Figure 3-31: Power flow of the area in 2040, Green scenario

From Figure 3-29, the total negative value $41,038\ MWh$ energy would flow to the grid, and the positive part, total $40,316\ MWh$ should be bought from the grid. and the difference $722\ MWh$ energy could get subsidy. As a result, the energy distribution were shown as follows.

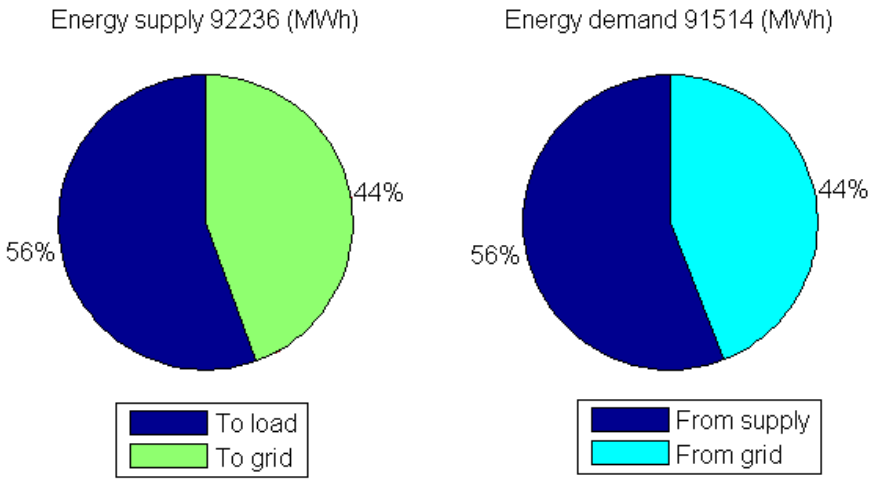

Figure 3-32: Energy distribution, Green scenario

Then, the electricity kilowatt-hour (kWh) price were calculated and listed below.

Table 3-11: Cost overview for Green scenario

Cost Fraction	Investment	Maintenance	Total €/year
Solar panel	130,413,368	521,653	
Wind turbine	57,600,000	345,600	
Inverter	22,952,753	229,528	
Energy subsidy			42,439
Electricity Cost	€0.1393/kWh		

3-8-2 Smart Scenario

For the Smart scenario, initially the total maximum yield energy would be $151,280\ MWh$, including $229,601\ m^2$ (25% of the roof area with 1.5% mismatch) solar panel ($100,733\ MWh$), 1510 small scale wind turbine ($13,911\ MWh$) and 24 large scale wind turbines ($36,472\ MWh$), and the total energy demand would be $91,514\ MWh$. The maximum energy supply could sufficiently match the energy demand in the aggregate, even though there still appeared energy shortage in winter. The value of seasonal part of the demand and supply were list below in detail and shown.

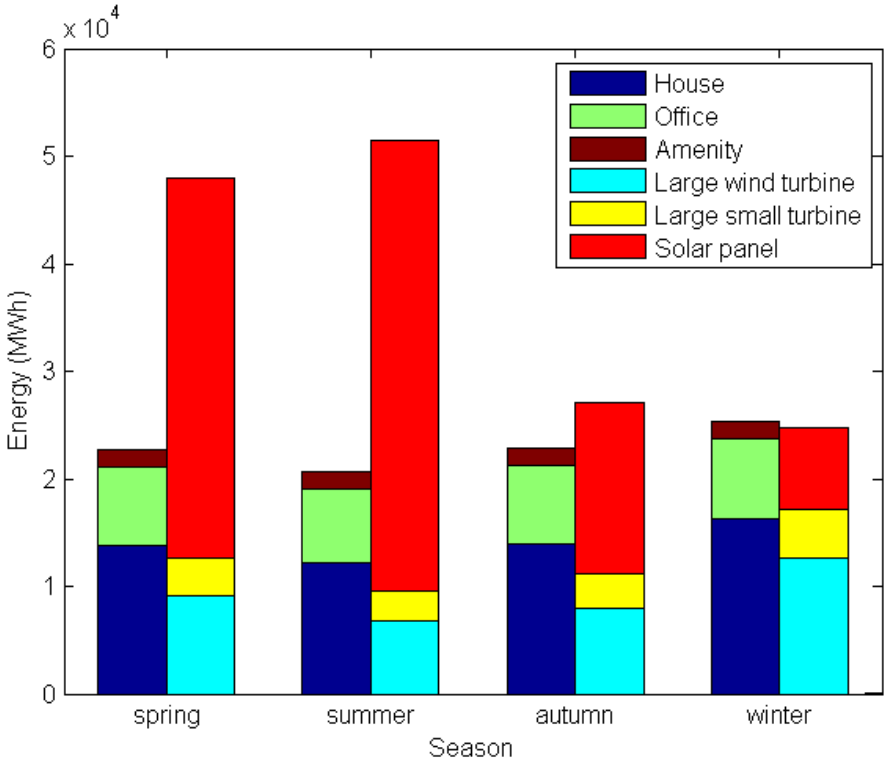

Figure 3-33: Energy balance between demand and supply in 2040, Smart scenario

Table 3-12: Energy balance between demand and supply in 2040, Smart scenario

	Supply (MWh)			Demand (MWh)		
	PV	WG (L)	WG (S)	House	Office	Amenity
Spring	35,299	9,127	3,478	13,784	7,318	1,588
Summer	41,953	6,752	2,803	12,224	6,898	1,472
Autumn	15,882	8,022	3,188	13,998	7,280	1,570
Winter	7,599	12,570	4,606	16,341	7,437	1,606

The percentage of each parts were changed and shown in Figure 3-24 below.

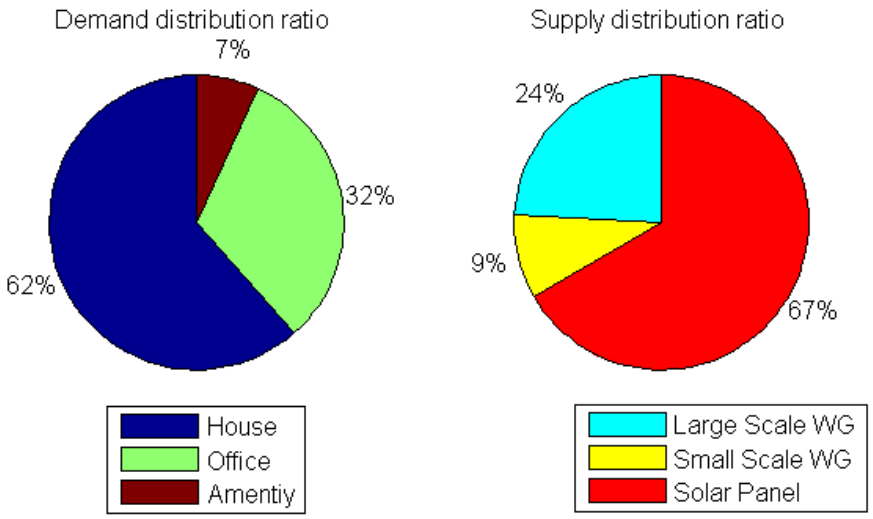

Figure 3-34: Energy distribution in 2040, Smart scenario

The yearly power flow was also simulated in detail.

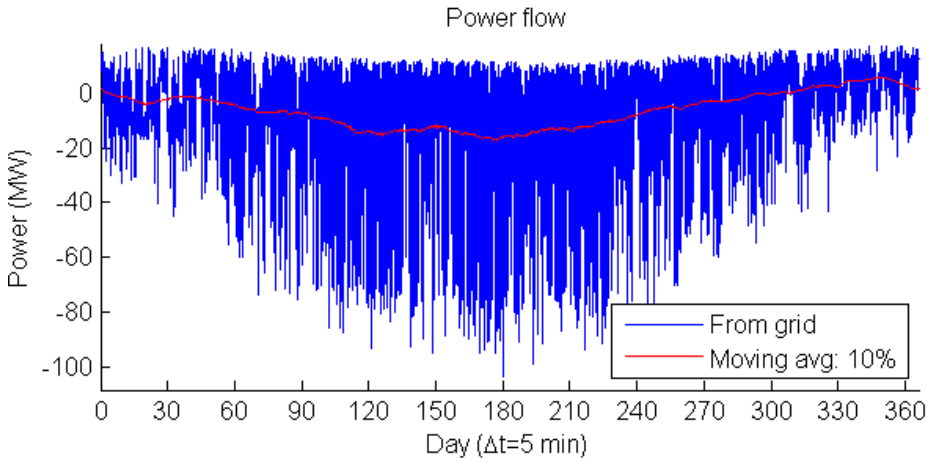

Figure 3-35: Power flow of the area in 2040, Smart scenario

From Figure 3-35, the total negative value $8,963\ MWh$ energy would flow to the grid, and the positive part, total $3,390\ MWh$ should be bought from the grid. and the difference $5573\ MWh$ energy could get subsidy. As a result, the energy distribution were shown as follows.

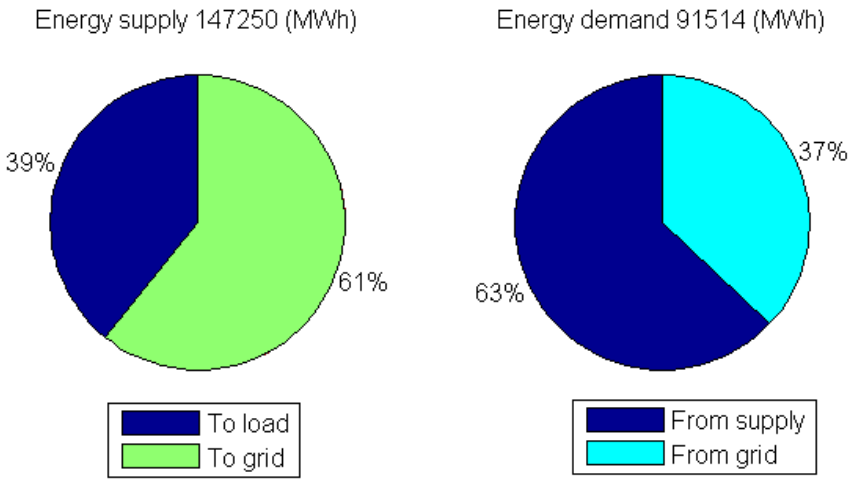

Figure 3-36: Energy distribution, Smart scenario

Then, the electricity kilowatt-hour (kWh) price were calculated and listed below.

Table 3-13: Cost overview for Smart scenario

Cost Fraction	Investment	Maintenance	Total €/year
Solar panel	229,601,000	918,404	
Wind turbine	74,028,800	444,173	
Inverter	40,409,776	404,098	
Energy subsidy			3,277,295
Electricity Cost	€0.1935/kWh		

With the same iterative algorithm, the optimal result in Smart scenario was the same as the optimal result in Green scenario, which meant the supply in this scenario could be reduced to the same scale. The small wind turbine would be removed and the solar panel would be reduced from $229,601\ m^2$ (25% of the roof area with 1.5% mismatch) to $130,413\ m^2$ (14.2% of the roof area with no mismatch), so the result did not show again here.

3-9 Summary

In this chapter, the load models in different season were shown at first. Then the yearly energy models are ideally established combing these daily profile. After the individual demand and supply were revealed and combined based on the urban indicator documents, two scenarios were presented in this study. Although two scenarios were totally different, e.g. the area of solar panel and the number of small wind turbines, the maximum number of the large wind turbines were the same.

Upon completion of simulation of the Green scenario as an example, it was indicated that the maximum energy supply could meet the demand in aggregate, and seeing the yearly power flow in detail, a battery storage system is introduced at first. By considering the price and size of the battery needed, it was suggested that the electricity transaction in different time could be an alternative. but only with the battery, the energy balance still can not meet in all times. The extra energy was needed from the grid.

Based on the analysis on the cost, a cheaper electricity price was also preferred, which could also reveal the efficient use of the energy. the investment cost was obtained. The energy which could not use directly and flow to the battery would cause transmission loss. After reducing the battery, it shown that the electricity price dropped very much. and the energy sold to the grid were also with a lower price, so the supply device could also be adjusted.

Finally, the optimum scales of the supply device in two scenario were determined, and the optimal result in both scenario were the same. The both scenario could achieve the energy neutral with the help of the surrounding grid.

EV was a prime in a sustainable city for battery charging. With increase of the individual battery rating and the number of EV's, the charging load could be add to the total energy demand from the grid point of view. As such, the smart grid with EV charging will be discussed in the next chapter.

Chapter 4

EV Charging System

4-1 Introduction

The electric vehicle is another important part in the sustainable city, which powered by stored electricity originally from an external power source. And these electricity should be replenished from an external power station. These electricity consumption will increase the previous energy demand and the energy supply will also increase correspondingly. Based on this situation, firstly the EV number and the average daily consumption need to be assumed which can estimate the total increasing energy demand. Then the different charging methods are proposed to show in detail, each of them have the different charging power and charging time. Finally the charging strategy as the most important element should be determined. Using a optimal charging strategy and combing with the different charging methods, it can not only influence the energy demand distribution, but also improve the grid power.

In the chapter, the additional EV charging system will be described step by step based on the analysis above. The renewed different scenario result will demonstrate with the same optimization analysis shown in Section 3-7.

4-2 Travel Pattern

The travel pattern is crucial to the estimation of the charging load of an EV. Due to the lack of real data, it was assumed to be consistent with others in the Netherlands[22]. Furthermore, the maximum driving distance of the EV currently available in the market is 160 km. For the up-to-date battery technology, the energy of average driving distance of EV was 0.175 kWh/km. Referring to the the initial scenario of 4,000 EVs, the daily charging load could be calculated. The 2009 travel pattern in the Netherlands which investigated by the previous researches was shown in Figure 4-1.

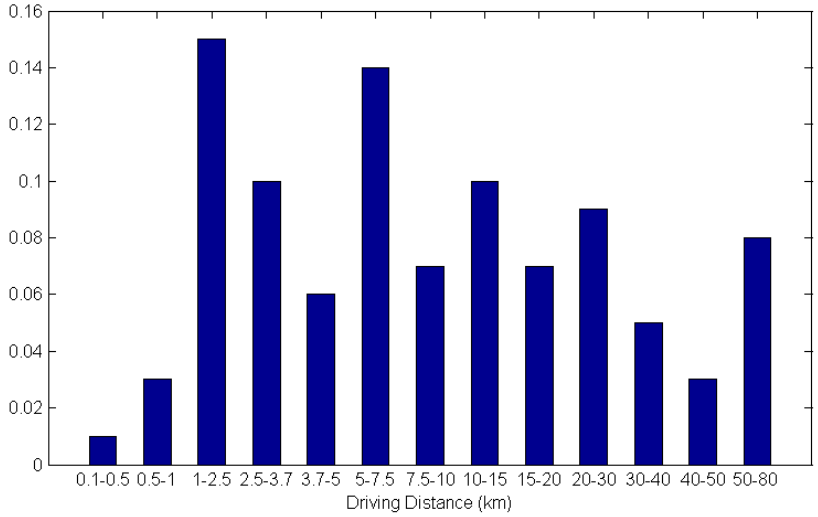

Figure 4-1: Traffic pattern - distribution of driving distance in the Netherlands

The travel pattern in Stadshavens area could be deduced form the figure. The average driving distance in Stadshavens was calculated as 16.58 km in one way trip. By combining the above information, the total daily load of electric vehicles was 23.2 MWh, which meant the previous optimum supply device scale could not meet the total energy demand. So, the solar panel and wind turbine would adjust again.

Inclusively the travel pattern in the Netherlands, the user groups of parking places in Stadshavens was first assumed. As the household distribution above-mentioned, there were half of the vehicles could park in the working area in 2040. Then the vehicle users could be assumed and classified into local and commuting groups, listed in table 4-1.

Table 4-1: Assumption of EV user group

Group	Explanation	Percentage
Local	People that live in the area (charging at night in weekdays and whole day in weekends)	50%
Commuting	People that drive to the business park (which arrives at 9:00 and leave 17:00)	50%

4-3 Charging Method

The EV charging method would influence the peak of the energy demand. Referring to the standards, they could be classified into three categories, i.e., slow charging, medium charging and fast charging (see Figure 4-2). To make a reasonable estimation on the charging load of EV in a specific year, the assumptions of the concurrency of EV charging were pinpointed.

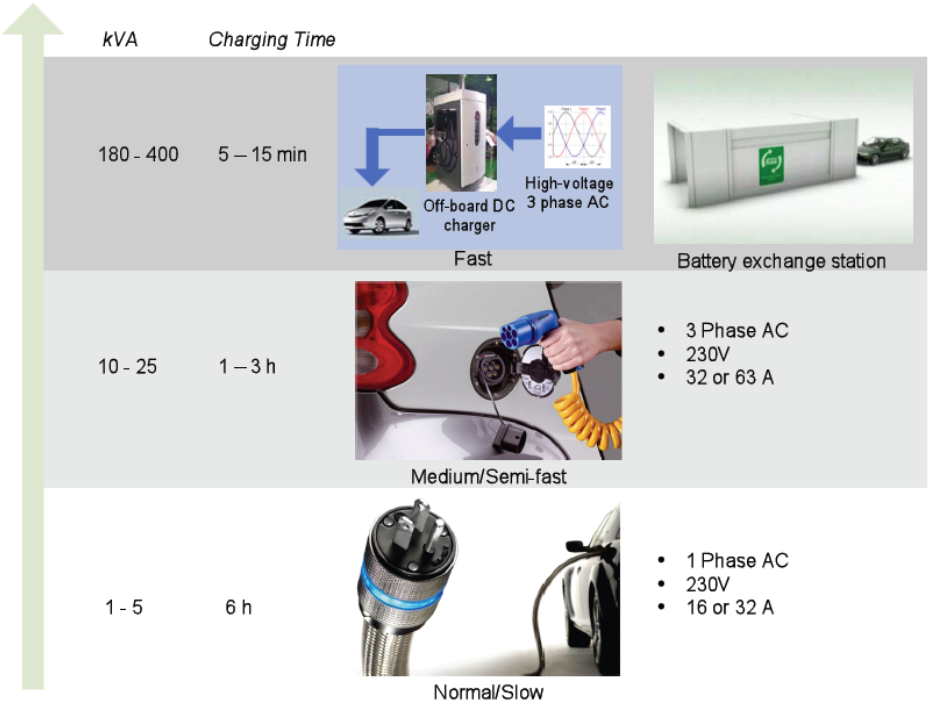

Figure 4-2: Charging modes of EV, source: Schihpol the Grounds 2030

The fast Charging was provided by an off-board charger with DC, viz., the charger converted AC power to controlled DC power so as to charge the EV battery. This solution was frequently used for fast charging stations requiring such a heavy infrastructure that was limited to public charging stations. The charging time required to fully charge a battery was from 5 to 15 min. The power peak of this charger station was situated around $50-75\ kW$. Therefore, fast charging was unlikely to undertake simultaneously. The total number of fast charging stations would be limited with 1% concurrency.

The medium/semi-fast charging, which applied a charging power of 22 kW, corresponded to a three phase 32 A outlet. A semi-fast charging infrastructure allowed a charging time between 1 hour to 3 hours for a 30 kWh battery. This type of infrastructure was directly connected to an AC supply network and used at a public location. The medium/semi-fast charging was unlikely to exist concurrently. However, its concurrency was assumed to be higher than the fast charging as 10%.

The slow charging, also called standard charging, was defined as a power level of 3.7 kW, corresponding to a 230 V and 16 A socket-outlet. This type of single phase AC charger was extensively used in Europe and dedicated to a normal charging time of 6-8 hours. Due to its simplicity and low cost, it was proffered to applying at a private location, such as household and workplace. The probability of concurrently slow charging was high, because most resident vehicle drivers were likely to take advantage of the low electricity cost after 11:00 p.m.. The percentage of EVs charging at the same time was assumed to be 89%.

4-4 Charging Strategy

The charging strategy was closely related to the charging group and charging time, further influenced the energy demand distribution. Initially, three charging strategy were assumed and simulated using average daily profile in weekday and weekend respectively for parking group. After comparing the pros and cons of the results, an optimal charging strategy was chosen.

4-4-1 Dumb Charging

In weekdays, for the commuting user group, it was ensured that the EVs were charged up to at least the daily consumption before departure in the afternoon. The charging time was therefore between 9:00 - 17:00, and the EVs were charged just after the arrival at the parking spaces. The medium and fast charging were not considered in this strategy, because the load of slow charging was emphasized in particular. For the local parking group, the EVs were charged just after the arrival at home (18:00). In weekend, the commuting user group does not appear in the area, so the energy they consumed could not charged again and should charge advanced in the weekdays. Then, only the local parking group was considered and the charging time was determined at beginning of the day. The load profile of the dumb charging was shown below.

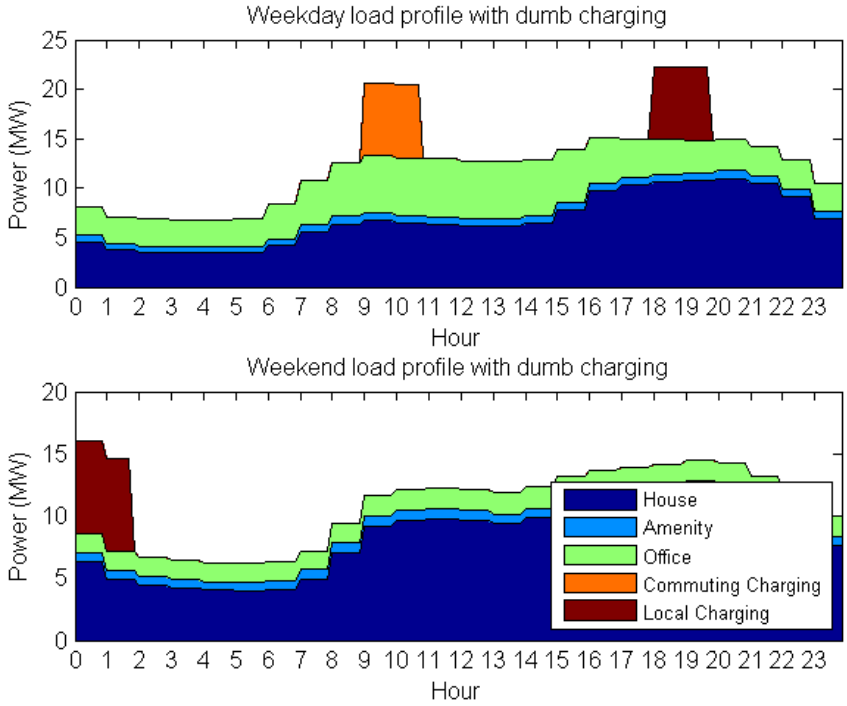

Figure 4-3: Daily load profile with dumb charging

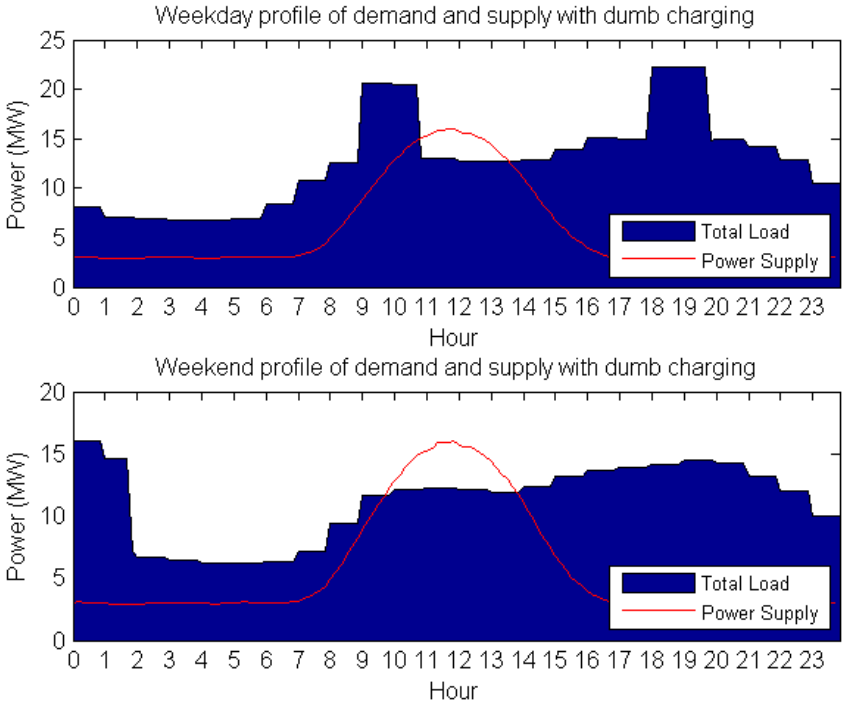

Figure 4-4: Daily profile of demand and supply with dumb charging

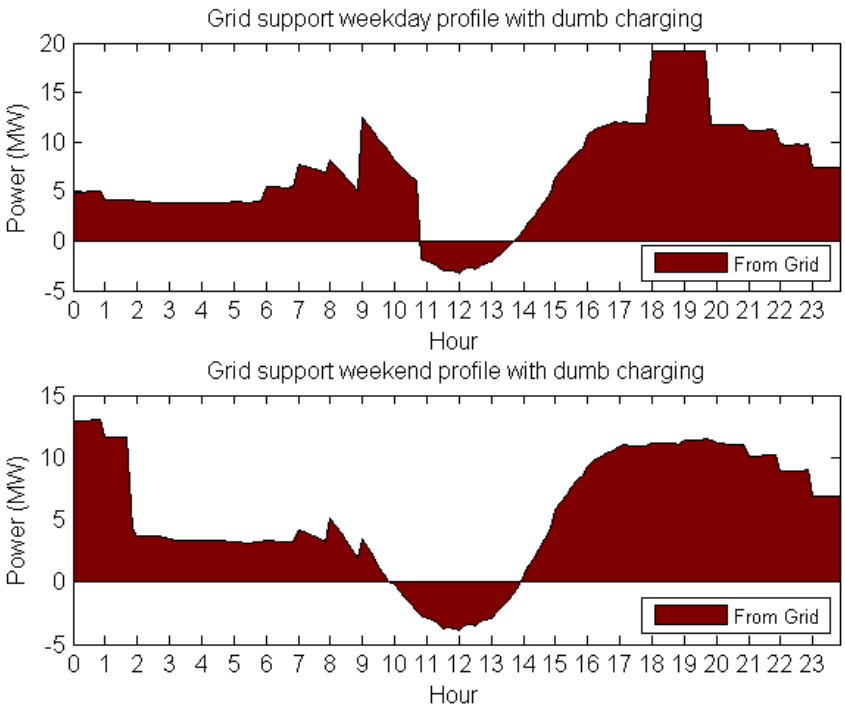

Figure 4-5: Power flow with dumb charging

From Figure 4-3, it was shown that with dumb charging the EVs were charged directly after their usage, without considering the grid limitation. The load of slow charging showed high power peak, due to the simultaneous charging of many EVs. The dumb charging option with slow charging was not acceptable. This is due to the following reasons. Firstly, the maximum load for charging was much higher than the total electrical load of Stadshavens without charging. The high peak power required a large update of the costly power network. Then, it produced other energy shortage periods, while the solar/wind production was sometimes higher than the load,as shown in Figure 4-4. It meant there was no help to the efficient energy usage. As such, the energy surplus had to be either sold to the grid at a low price or stored with loss.

4-4-2 Controlled Charging

Further elaborated, if the charging of EVs could be controlled using the appropriate charging mode, the abovementioned shortcomings would be avoided. In weekdays, for the user group, charging was evenly distributed during the charging time. Due to the necessity of vehicle usage in the working time, the medium and fast charging was considered, i.e. 10% and 1% of the commuting user group between 9:00 - 17:00 in working days. The number of fast charging stations was assumed as two in this study. This was because 1% of the EVs in the commuting group needed fast charging, and the number of fast charging stations should be constrained as low as possible. In weekends, the local parking group charged evenly in the whole day.

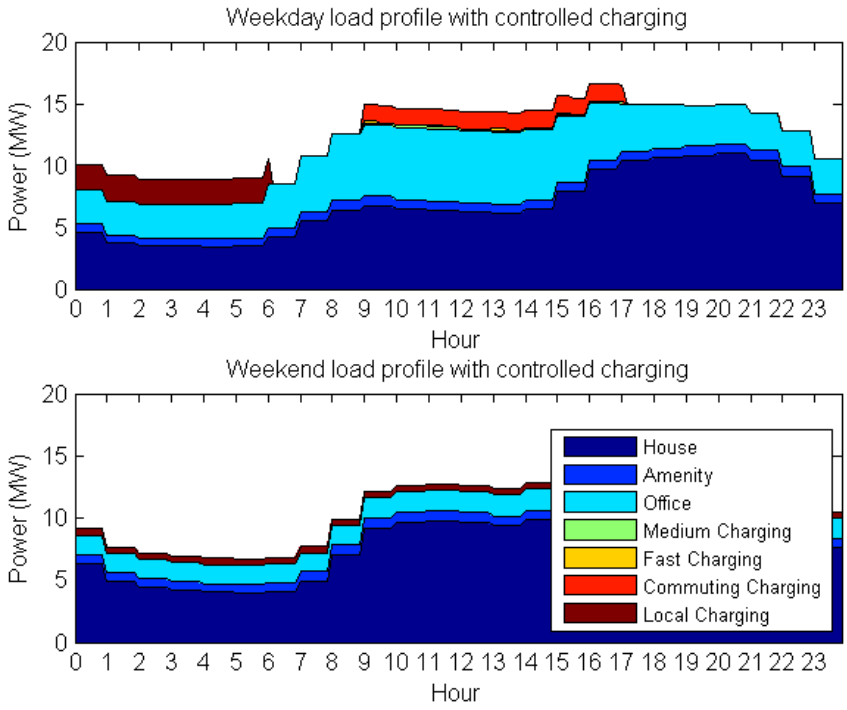

Figure 4-6: Daily load profile with controlled charging

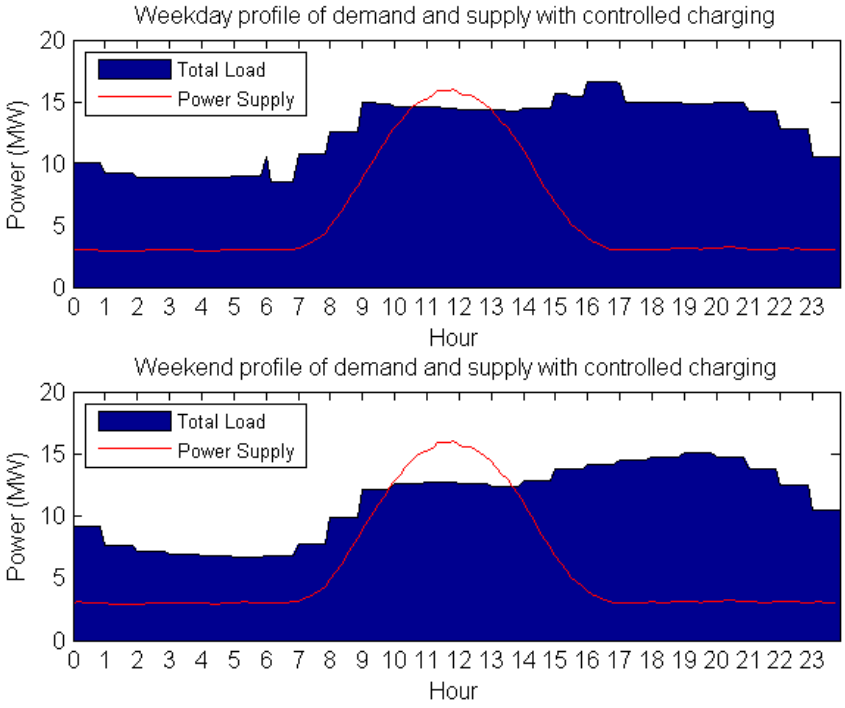

Figure 4-7: Daily profile of demand and supply with controlled charging

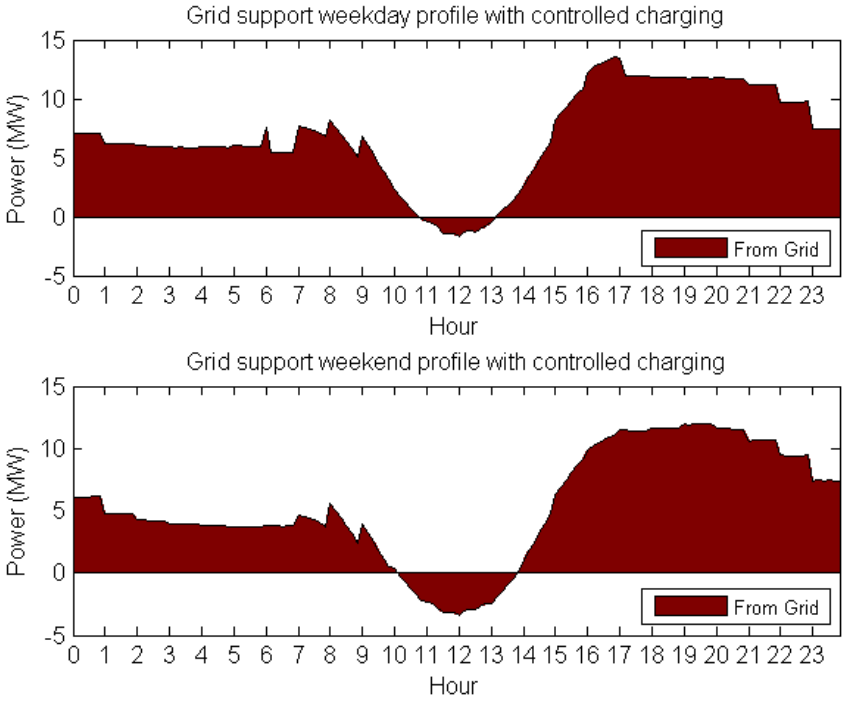

Figure 4-8: Power flow with controlled charging

For controlled charging, the slow charging of EVs was distributed evenly across the possible charging period. Compared with the dumb charging, the power peak was limited and the power supply fitted the electrical load during weekdays better, viz., controlled charging was a much better option. For fast charging, it was considered upon limited fast charging stations, i.e., 2 in this study. Hence, its peak power was under an acceptable level, whereas the power flow was not smooth in the whole week. So far, the smart charging method was proposed to resolve this problem, and discussed in the next section.

4-4-3 Smart Charging

In the smart charging option, the charging of EVs was controlled to absorb surplus energy[23]. By doing so, the peak power was limited and the power flow could be more smooth. Therefore, smart charging not only distributed the charging load, but also improved the economical efficiency of solar/wind power production.

For the commuting group, the medium and fast charging pattern was the same as that of controlled charging. The slow charging pattern was conducted by smart charging with consideration to the grid limitation, viz., improving the grid integration of renewable energies. For the local group, the smart charging was used at weekends.

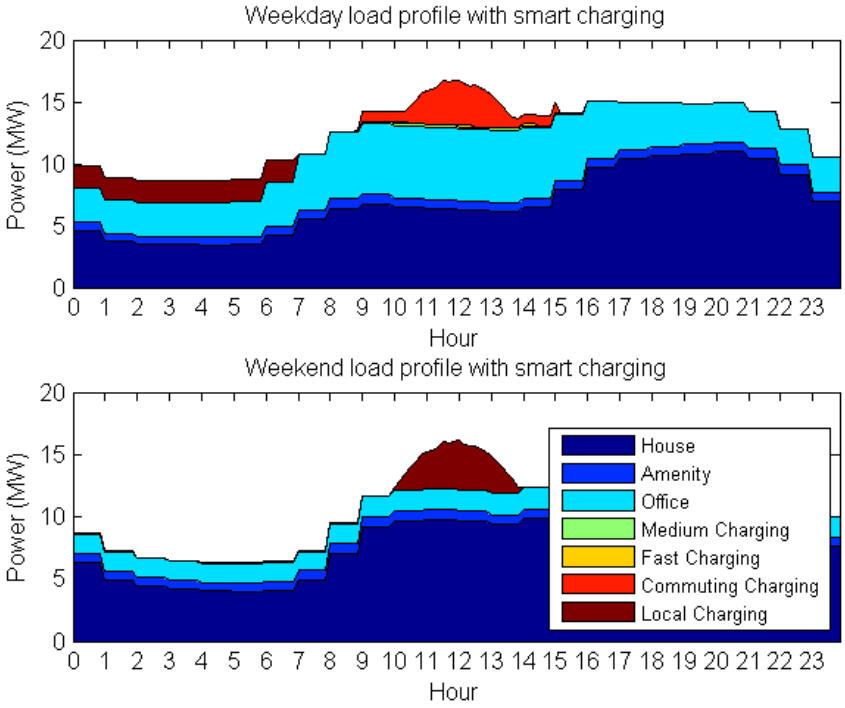

Figure 4-9: Daily load profile with smart charging

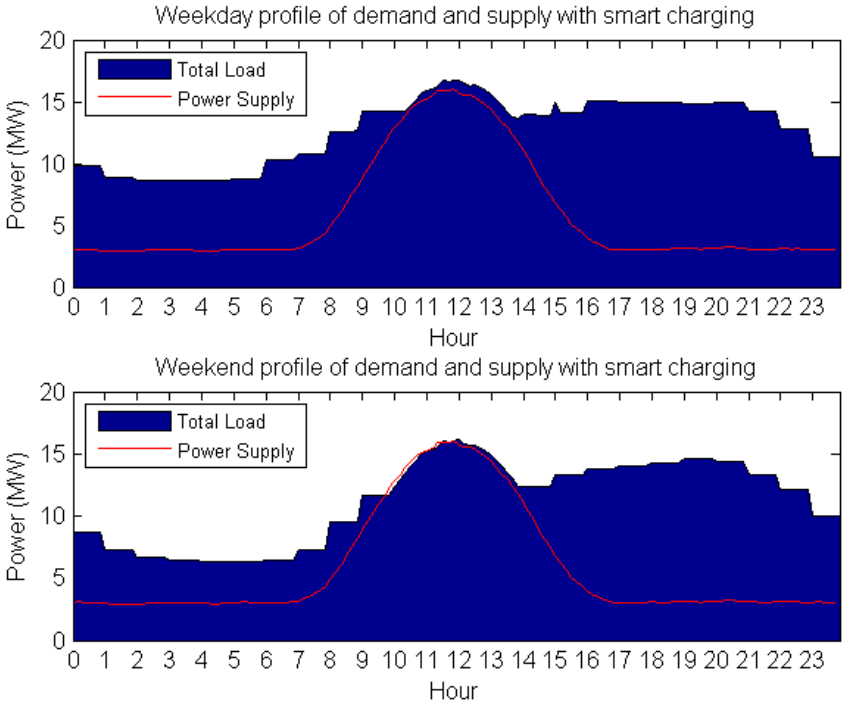

Figure 4-10: Daily profile of demand and supply with smart charging

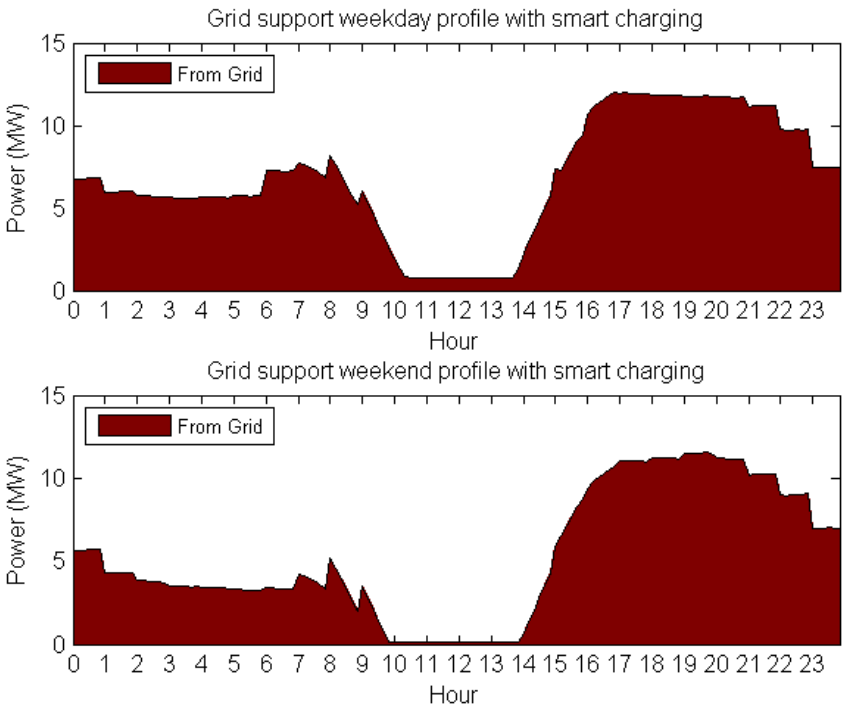

Figure 4-11: Power flow with smart charging

In weekdays, the local group charged evenly before daybreak, when the electricity load was low. For the commuting group, the medium and fast charging was evenly distributed in the oversupply daytime. The load of slow charing was divided into two parts: one was to absorb the abundant energy and the other was evenly distributed in the working time of 9:00 - 17:00 if the abundant energy was not sufficient. In weekends, the local group was charging in smart pattern with energy surplus in the whole day and a low-level of the peak power. In all, it was concluded that the smart charging could absorb the abundant power, limit the power peak, decrease the power loss, and increase the economic efficiency.

From Figure 4-9, it could be seen that even the local group charging at night in weekdays, it would still increase the energy demand, while in the weekend the commuting group would not drive to the office, the charging load would be lower in the weekends. On the other hand, the building load would also lower in the weekends, which meant the energy redundancy was higher in the weekends.

In order to eliminate the weak point of the smart charging strategy shown in the daily situation above, the charging cycle would be extend to one week as a period. And the simulation object were changed from weekdays and weekends to the commuting and local parking group.

For the commuting group in weekdays, they would charge in working hour (9:00 - 17:00), the fast and medium charging are evening distributed. the slow charging would be divided into two parts, it would first absorb the superfluous energy to reduce the power peak in the charging time, then if these energy were not sufficient, the remaining part were also evening distributed in the charging time. The energy consumption they used to drive in weekends would be charge in advance during the energy redundancy time in the weekdays.

For the local group, since there were not energy redundancy in their previous charging time at weekday night. The energy consumption they used to drive in weekdays would be concentrate to charge in the weekends during the energy oversupply time. If these superfluous energy were not sufficient, the remaining part part would still charge evenly in the previous charging time at night.

Based on this strategy, the smart charging would be adjusted and simulated on weekly period. The result of four week in different season results were chosen and shown in detail as follows.

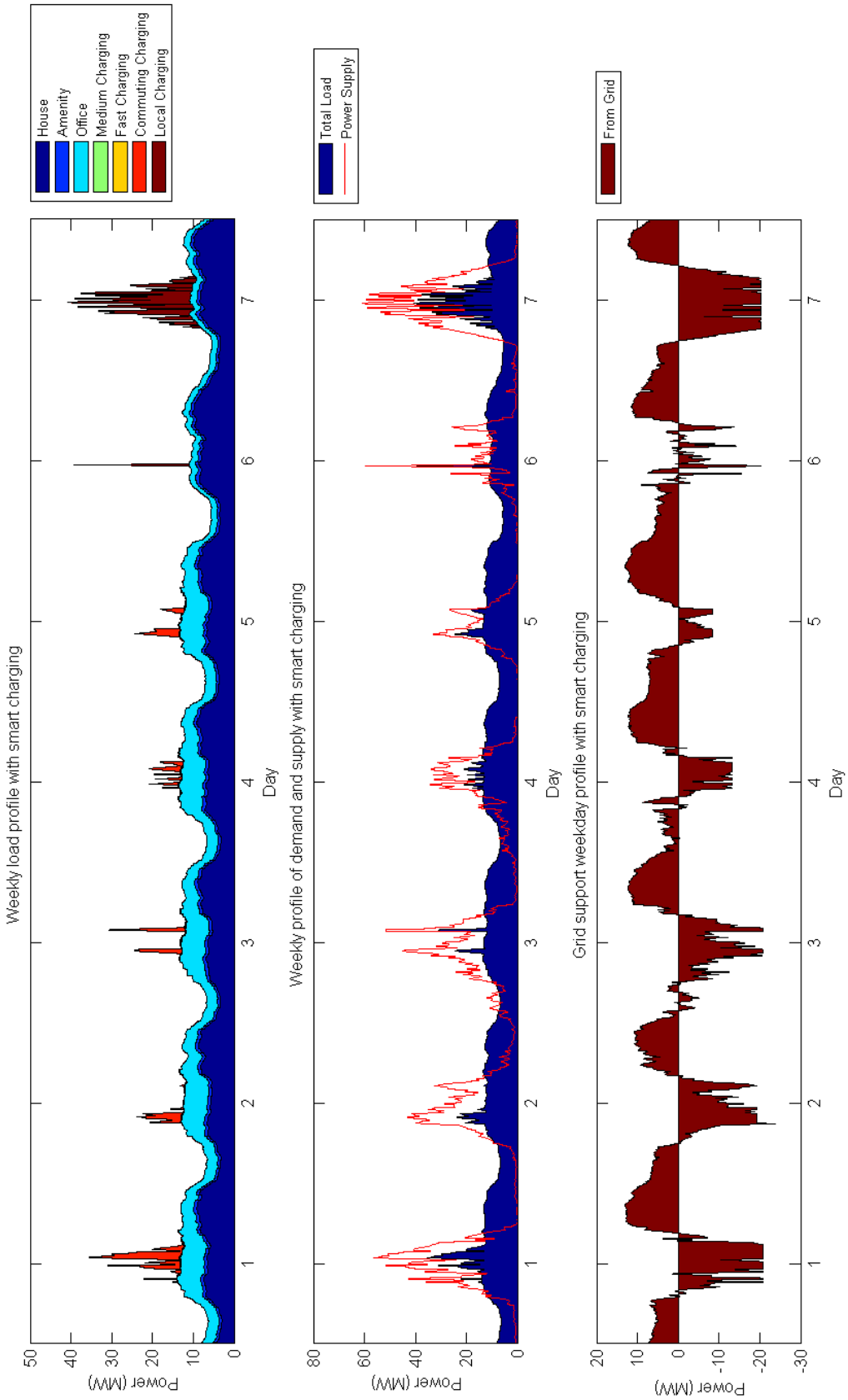

Figure 4-12: Week 14 load profile with smart charging in spring, Green scenario

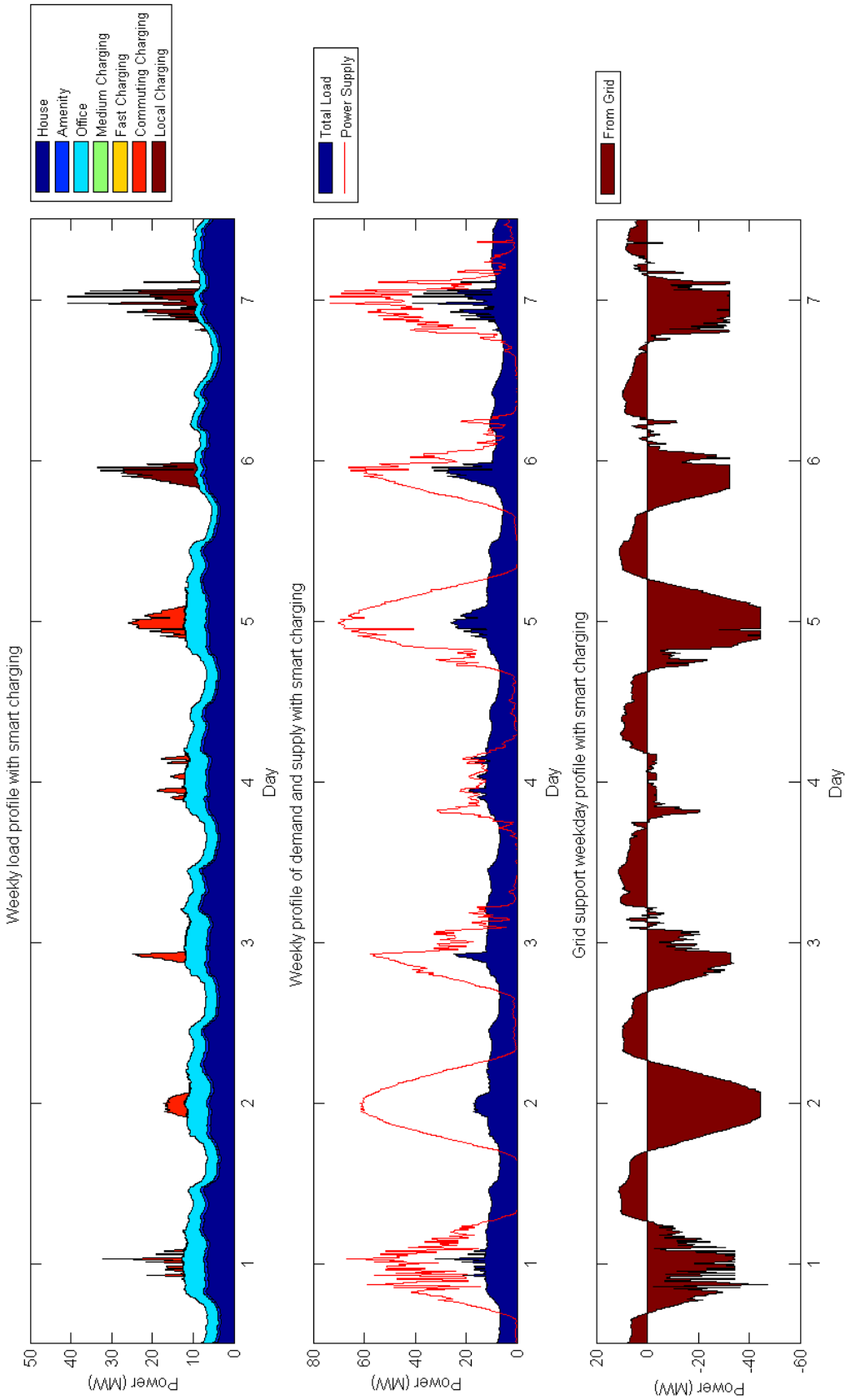

Figure 4-13: Week 27 load profile with smart charging in summer, Green scenario

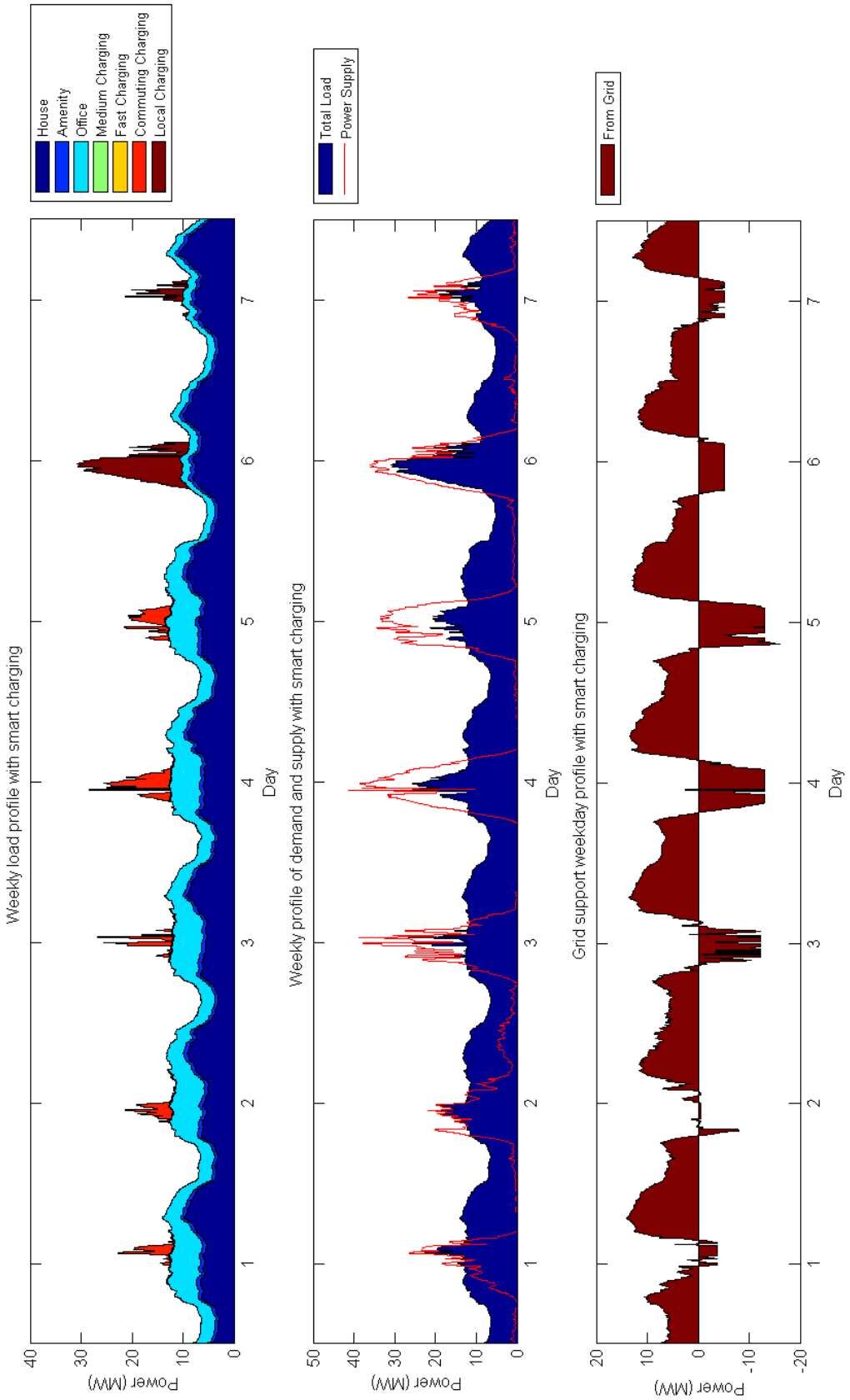

Figure 4-14: Week 41 load profile with smart charging in autumn, Green scenario

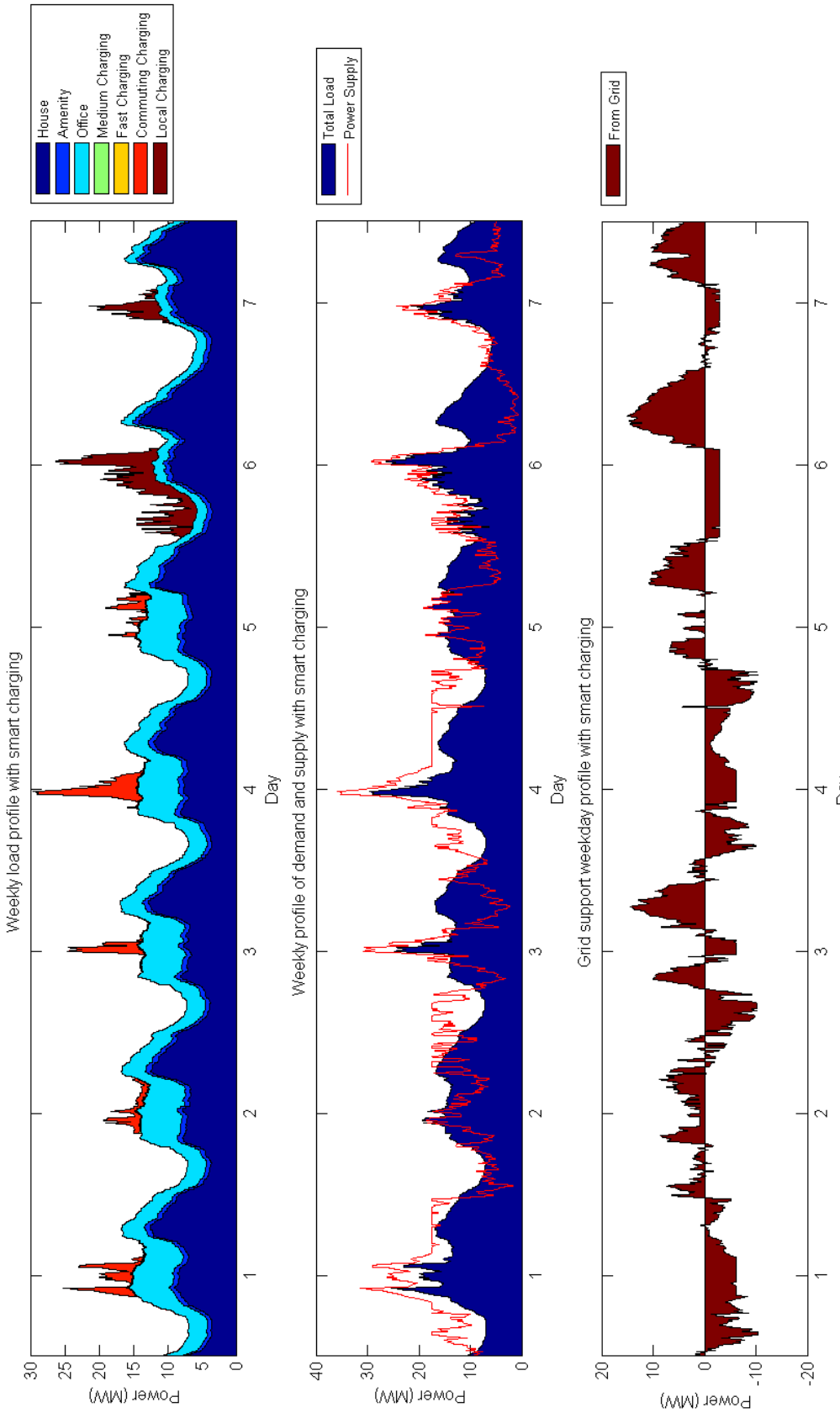

Figure 4-15: Week 2 load profile with smart charging in winter, Green scenario

From the figure above, the improved smart charging was an optimal choice to charge the vehicle. Choosing a flexible charging time meant the EV could always charge at energy oversupply time. This charging strategy could reduce the power peak and smooth the power flow.

4-5 Storage Analysis

Since the daily vehicle energy consumption only occupied a small part in the total vehicle battery capacity, the battery in the electric vehicle could also be treated as the storage media, it was possible to shift the energy, which could also improve the energy usage. Unlike the liquid metal batteries deployed to support the electric grid. Several different types of battery were commonly used in electric vehicle, including: lead-acid, Nickel Metal Hydride (NiMH), zebra and Lithium ion (Li-ion). Considering the the drawback of these battery, viz.that lead-acid had lower energy density, NiMH battery with less efficientand , zebra needed to heated for use and also had poor power density, while lithium ion had a short cycle lives. Lead acid batteries were still the most used form of power for most of the electric vehicles used today, and its efficiency (80%) was used in this project.

As initial assumptions, the energy of average driving distance of EV was 0.175 kWh/km. The individual average daily travel energy was then calculated as 5.8 kWh. As aforementioned, the capacity of the battery in one electric vehicle was averagely 30 kWh, so the lowest state of charging (SOC) a driver wanted in his car at all time was calculated as 20%. With the total 4000 vehicles in the area, supposed that the commuting parking group was not always in the area, e.g. driving to the office and living outside the area, the stable local parking group (50%) would be used as part of the storage system. As such, except for the electric vehicle charging, 50 MWh could be used to store and shift within one day.

Reviewed the previous chapter, the assumed 200 MWh battery could only store 5% energy redundancy, which could be inferred the effect of these vehicle battery would very small and could be neglected.

4-6 Scenario Result with EV

The introduction of the electric vehicle would increase the energy demand, so the energy supply could increase compared with the scale which optimized in the previous chapter. Based on the daily load of electric vehicle 23.22 MWh and the roughly relation between energy via grid and ratio of supply/demand which shown in Figure 3-28, the energy balance was updated.

Through the iterative algorithm, the optimal results in two scenario were still the same. The total yield energy would be $105,735\ MWh$, including $165,313\ m^2$ (17% of the roof area with 0.4%) solar panel ($69,264\ MWh$) and 24 large scale wind turbines ($36,472\ MWh$), and the total energy demand would be $102,136\ MWh$. By using these amount of energy producing, the load demand was matched. Then, the seasonal matching result in 2040 was also shown in Figure 4-16, and listed in table.

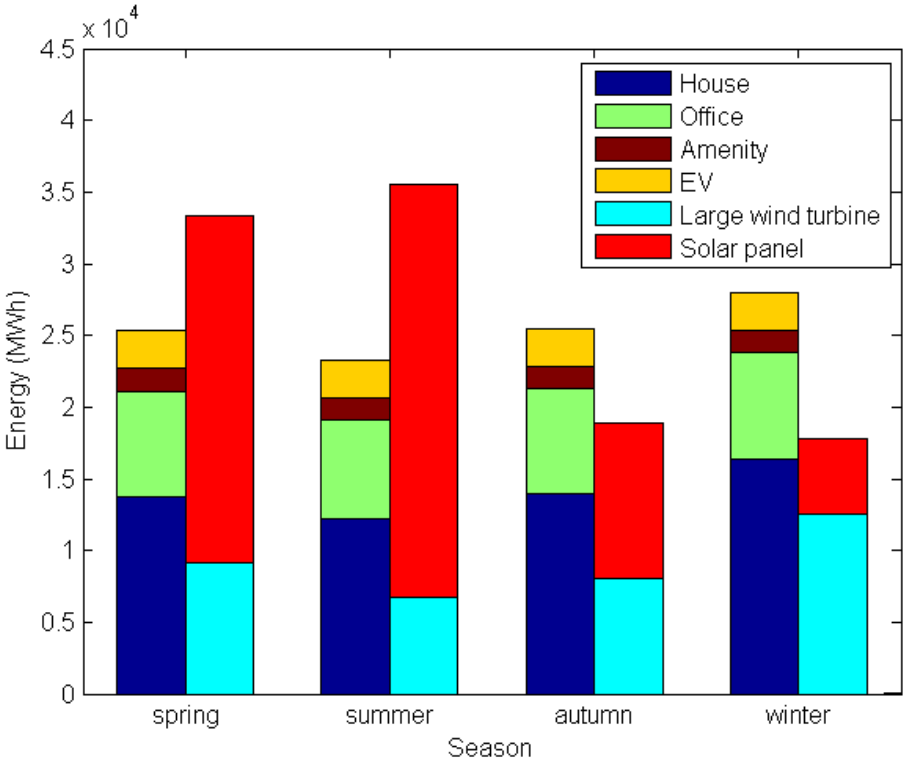

Figure 4-16: Energy balance between demand and supply with EV in 2040

Table 4-2: Energy balance between demand and supply in 2040

	Supply (MWh)		Demand (MWh)			
	PV	WG (L)	House	Office	Amenity	EV
Spring	24,272	9,127	13,784	7,318	1,588	2,670
Summer	28,847	6,752	12,224	6,898	1,472	2,670
Autumn	10,920	8,002	13,998	7,280	1,570	2,641
Winter	5,225	12,570	16,341	7,437	1,606	2,641

The percentage of each parts were changed and shown in Figure 4-17 below.

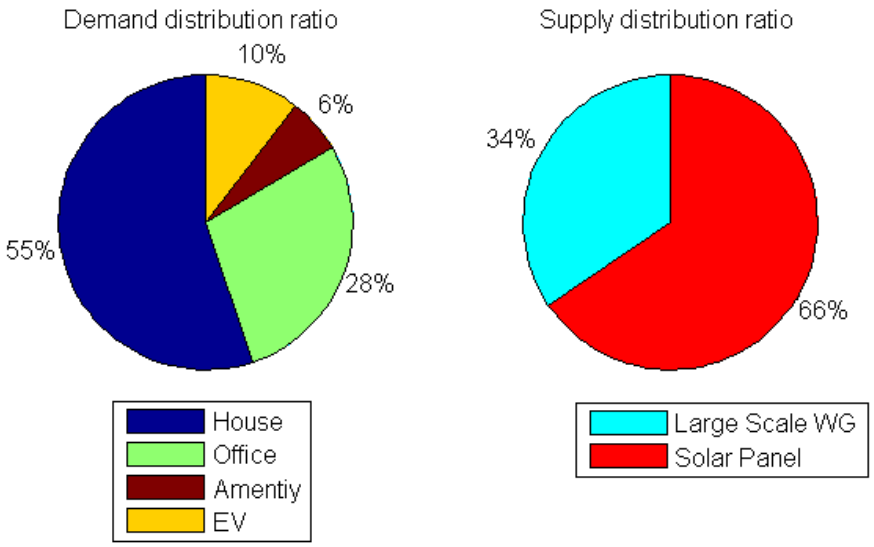

Figure 4-17: Energy distribution with EV in 2040

By considering all seasons, the maximum energy supply could sufficiently match the energy demand in the aggregate, even though there appeared energy shortage in autumn and winter. The yearly power flow should also be simulated and the vehicle would always charged at energy redundancy time. As a result, $40,103\ MWh$ energy would flow to the gird, while $39,275\ MWh$ should return back. The energy distribution were shown as follows.

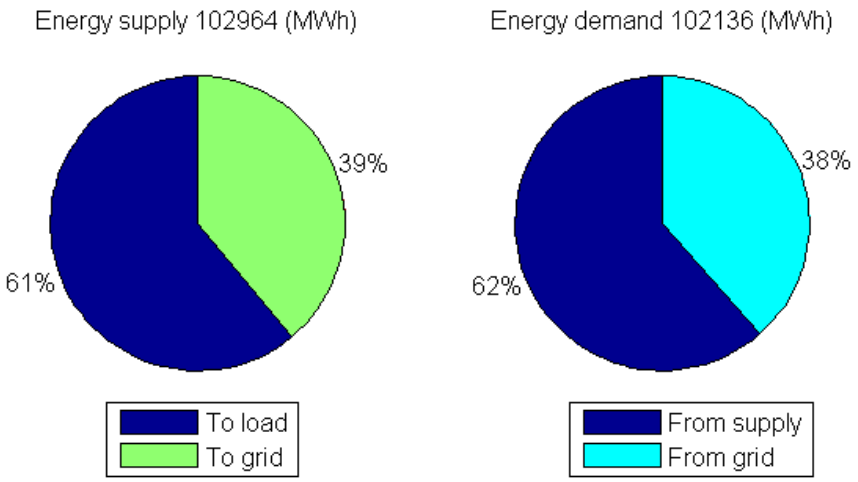

Figure 4-18: Energy distribution with EV

Then, the electricity kilowatt-hour (kWh) price were calculated and listed below.

Table 4-3: Cost overview with EV

Cost Fraction	Investment	Maintenance	Total €/year
Solar panel	155,504,165	622,016	
Wind turbine	57,600,000	345,600	
Inverter	27,368,733	273,687	
Energy subsidy			672,663
Electricity Cost	€0.1367/kWh		

4-7 Summary

Since the charging time and power could be controlled, the electric vehicle was generally recommended for providing a short term regulation function, as a sample, some EVs are often charged at mid-day. The charging can be controlled to flatten the noon load curve (reduce the load peak) or to improve renewable energy integration, which was obvious in summer.

Compared with the scenario without EV, After adding the EV, the energy demand increased, so the energy supply device also increased correspondingly. The supply could meet the demand in aggregate, the adding EV could absorb the energy redundancy, which reduced the energy flown to the grid. As a result, the €/kWh cost was cheaper than the cost without EV.

In all, even though the EV charging could increase the demand, the peak power to the grid was reduced. The energy exchange via the grid also reduced, which meant its dependence on the surrounding area is lower.

Chapter 5

Scenario Comparison

In the previous chapter, the different scenario and with or without EV were analyzed and optimized. In this chapter, the result of each situation were shown altogether to make some comparison.

First, the different situation without the battery storage system would be defined to show the difference.

- A. Green scenario with maximum energy potential
- B. Smart scenario with maximum energy potential
- C. Green/Smart scenario without EV through optimization
- D. Green/Smart scenario with EV through optimization

Then, some important parameters in different situation were list in table below.

Table 5-1: Scenario Comparison

	A	B	C	D
Energy Demand (MWh)	91514	91514	91514	102136
Energy Supply (MWh)	235604	151280	94559	105735
Solar Panel Percentage	82%	67%	61%	66%
Solar Panel Area (m^2)	192262	229610	130413	165313
Solar Panel Mismatch	6%	1.5%	N/A	0.4%
Large Wind Turbine Percentage	15%	24%	39%	34%
Wind Turbine Number	24	24	24	24
Small Wind Turbine Percentage	3%	9%	N/A	N/A
Wind Turbine Number	998	1510	N/A	N/A
Peak Power to Grid (MW)	180	105	59	45
Energy Flow to Grid (MWh)	169819(75%)	89632(61%)	41038(44%)	40103(39%)
Peak Power from Grid (MW)	17	17	17	17
Energy Flow from Grid (MWh)	33419(37%)	33896(37%)	40316(44%)	39275(38%)
Investment Cost (€)	608479792	344039576	210966121	240472898
Maintenance Cost (€)	3055754	1766675	1096781	1241303
Energy Subsidy (€)	8020332	3277295	42439	672663
€/kWh	0.3224	0.1935	0.1393	0.1367

Compared Green and Smart scenario from the table (row A and row B), it was clear that the Green scenario could produce more renewable energy, which meant it had a better expansion space.

Compared the result with and without optimization (row A,B and row C), it could be found that, the electricity price reduced dramatically, even the energy plow from the grid had been increased. Since the more energy production need more energy supply, and it would cost more investment expense, and the energy which could not plow to the load would be sold to the grid with a low price.

Compared the optimal result with and without EV (row C and row D), it shown that the €/kWh cost with EV was cheaper than the cost without EV. The energy demand increased when adding EV, the energy supply device also increased correspondingly, but the ratio of the energy supply and energy demand kept the same value. The adding EV could absorb the energy redundancy, which reduced the energy via the grid. On the other hand, it decreased the dependence on the surrounding area.

Chapter 6

Conclusions and Recommendations

6-1 Conclusions

This study was focused on the smart grid powered by wind and solar energies. Meanwhile, the feasibility of an existing urban area was speculated by using Stashavens as a case. Accordingly, the simulation on the potential energy was conducted, implying that the energy demand could be met with assistance of batteries and extra energy from the grid. Furthermore, it was found that by selecting a suitable charging mode and time of EV, it could improve the power flow, reduce the power peak.

· Analysis on the Energy Demand and Supply

Pertaining to the load profile, e.g. the building type and the number of area, a more comprehensive load model was proposed and established and simulated. In this regard, the amount of intuitive power consumption could be used for suitable selection of energy supply. Owing that the solar irradiance and wind speed were critical to the energy potential, the solar production was calculated based on the restrictions of the proposed area and such optimal installing parameters as GCR. And upon completion of height corrections, the wind energy production was determined. Thus the total maximum energy production were obtained.

· Analysis on the Energy Balance

The power flow balance regarding the energy demand and supply was investigated based on four-seasonal changes, and the ratio of solar over wind powers was uncertain. By calculating the maximum energy production, the yearly power flow was first presented via the storage system to shift the superfluous energy and take into account the efficiency. Therein, it was found that there still some energy mismatch between energy supply and energy demand. This might be settled by extra power sources from other places. In addition, the cost was analyzed and used as the priority optimization standards. Then, the battery would be removed and the scale of the supply would be adjusted.

· Analysis on the EV Charging

Although the EV charging was an energy-intensive approach, limited number of EV would not increase the energy demand very much. After comparing the different charging method and choosing a smart charging strategy, it allowed EVs to provide power to help balance loads by valley filling and peak shaving. It could also provide regulation services (keeping voltage and frequency stable), by storing excess energy produced during energy oversupply periods and providing it back to the grid during high load periods, thus effectively stabilizing the intermittency of renewable energy.

6-2 Recommendations

The goals of this thesis were aimed at testing and verifying the feasibility of the proposed model, i.e. building a suitable area, on the basis of real data. For the purpose of load profiling, a historical data was decomposed and referred in this study. It was clear that the energy supply could be rather different in a daily scale, due that the solar irradiance and wind speed were variated based on the some element like weather. Applying the historical values for real-time operation could result in inaccurateness. Based on this understanding, the prediction methods were employed by researchers to well address the real energy production so as to improve the daily real-time energy balance.

As above-mentioned in the study, the maximum energy potential was supposed. However, in some areas with sufficient energy in aggravate, it still remained problematic. Although the solar and wind energy possessed diverse distribution modes, the wind and solar resources were proven naturally-complementary. In this respect, enough solar energy was available during the day-time, whereas the wind energy was sufficient in the afternoon. Meanwhile, the solar and wind energies were adequately applied in summer and winter, respectively. Further elaborated, the solar energy was abundant while the wind energy was not enough due to the land constraints. In the future, another direction was to seek other renewable energy, which could make up the energy shortage in autumn and winter. This would also effectively resolve the randomness and intermittent of wind and solar energy. Accordingly, the continuous power could be provided to enhance the system's economic performance and operational reliability.

Similarly, due to the uncertainty of the power flow, the suitable charging time should be adjusted in a real-time manner to absorb the abundant energy or to release the energy towards the grid. This led to a complex real-time scheduling system to be established and managed.

Appendix A

Urban Plan

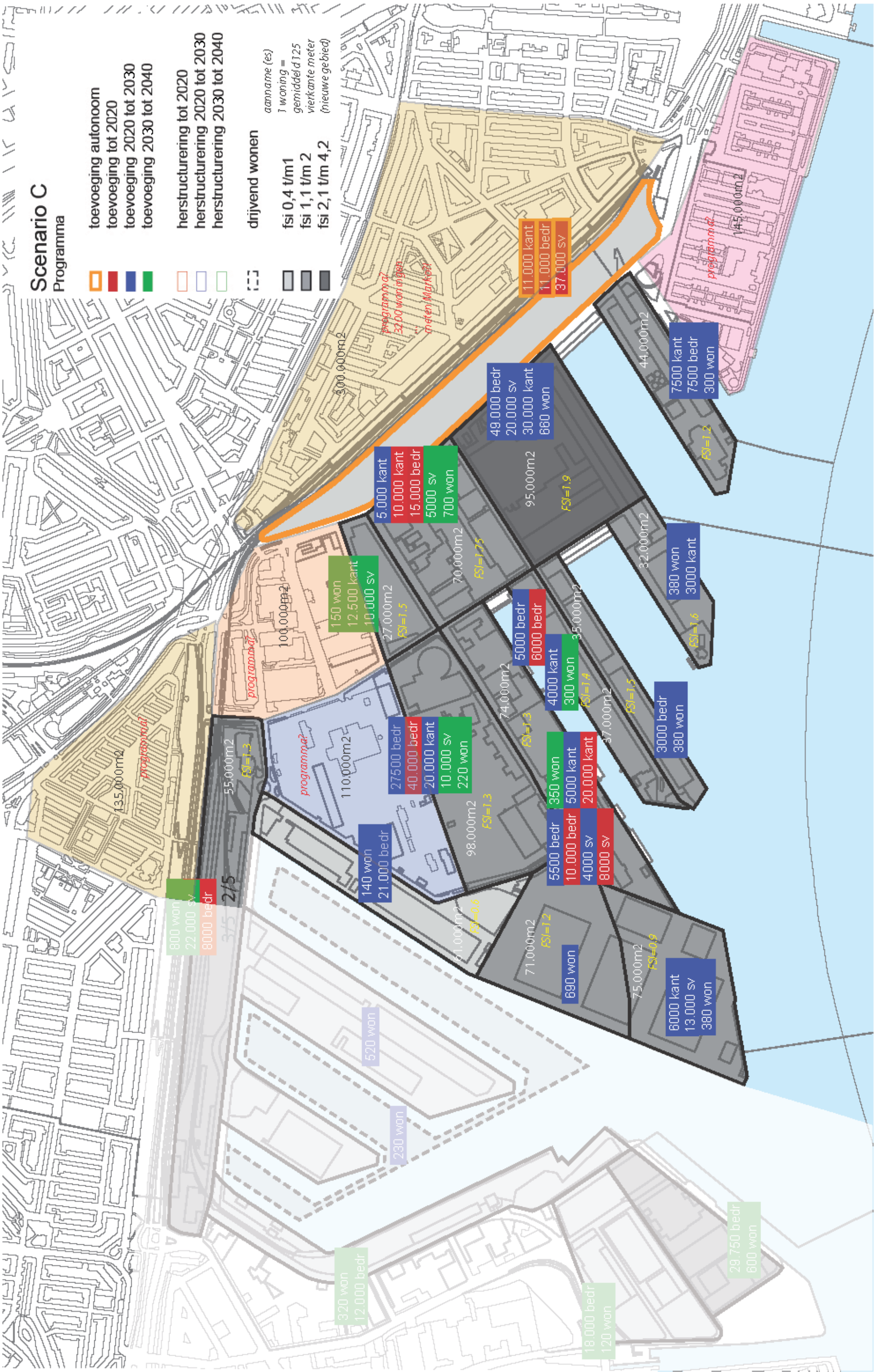

Figure A-1: Urban plan from 2020 - 2040

Appendix B

Daily Variations

B-1 Daily Variations in Solar Irradiance

Figure B-1 showed two randomly selected daily profiles in winter. In the downside figure, the blue lines showed the change in solar irradiance, which is the solar irradiance compared with the counterpart in the foregoing 10 minutes.

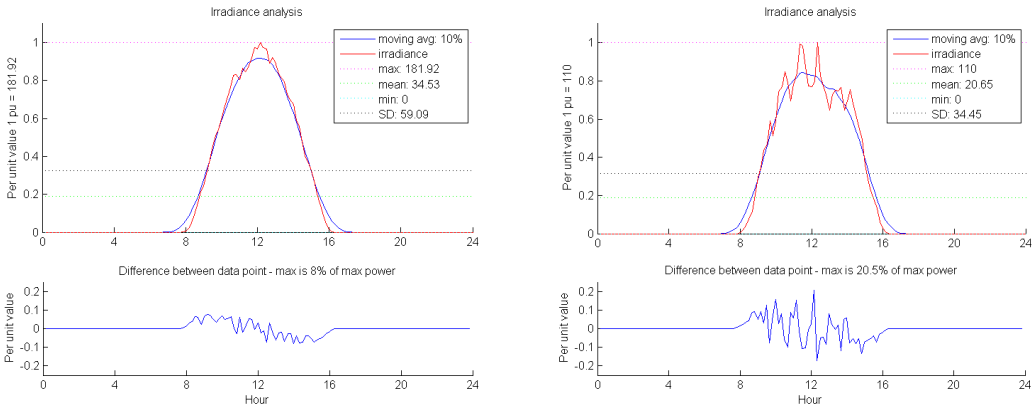

Figure B-1: Profile analyses of solar irradiance data, 2 days of the year 2010

It was clear that the peak and average value were all difference between these two days, but solar irradiance all increased from sunrise until midday, after which it decreased to zero at sunset, which was a regular variation. Based on this situation, the solar power was more predictable.

B-2 Daily Variations in Wind Speed

In real case, large variations in wind speed occurred during a single day, as could be seen in Figure B-2. The left figure showed one day with varying wind speed. The average wind speed during this day was about 0.53 (4.24/7.94) per unit (pu) max. The right figure showed another day when the wind speed was lower. The average was about 0.41 pu max.

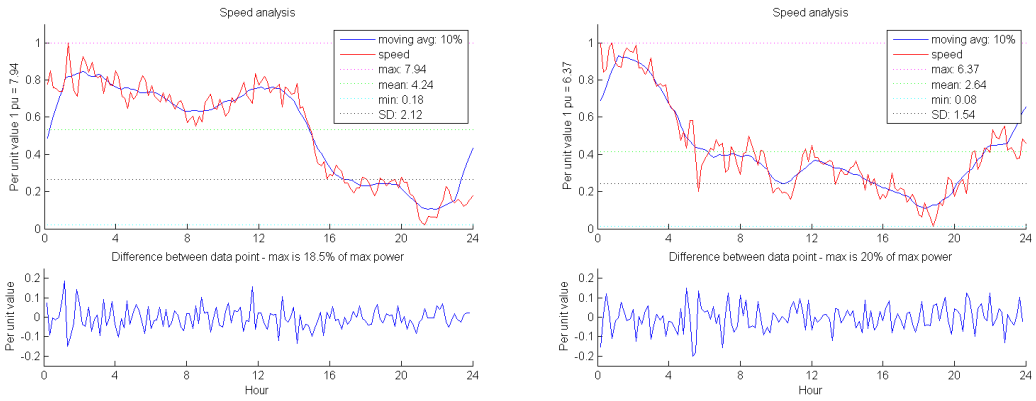

Figure B-2: Profile analyses of wind speed data, 2 days of the year 2010

The shapes of wind speed were all difference in two randomly selected winter day, which could be concluded that the real wind speed during a day differs almost always from the average 24 hour wind speed profiles. The blue lines indicated that the change in wind speed per 10 minutes was approximately over 10% of the maximum, which means it would change suddenly, so the wind speed was less predictable. So the average profiles were only used to get a better understanding of the variations to build the wind power model during the year.

Bibliography

[1] R. Register, *Ecocity Berkeley: Building Cities for a Healthy Future*. 1987.

[2] R. DeBlasio and C. Tom, "Standards for the smart grid," *2008 IEEE Energy 2030 Conference*, pp. 6–12, 2008.

[3] T. Markvart, "Sizing of hybrid photovoltaic-wind energy systems," *Solar Energy*, vol. 57, no. 4, pp. 277–281, 1996.

[4] M. A. Habib, S. A. M. Said, M. A. El-Hadidy, and I. Al-Zaharna, "Optimization procedure of a hybrid photovoltaic wind energy system," *Energy*, vol. 24, no. 11, pp. 919–929, 1999.

[5] W. Zhou, C. Lou, Z. Li, L. Lu, and H. Yang, "Current status of research on optimum sizing of stand-alone hybrid solar-wind power generation systems," *Applied Energy*, vol. 87, no. 2, pp. 380–389, 2010.

[6] A. Seppälä, *Load research and load estimation in electricity distribution*. PhD thesis, 1996.

[7] J. A. Jardini, C. M. V. Tahan, M. R. Gouvea, S. U. Ahn, and F. M. Figueiredo, "Daily load profiles for residential, commercial and industrial low voltage consumers," *IEEE Transactions on Power Delivery*, vol. 15, no. 1, pp. 375–380, 2000.

[8] L. Pedersen, *Load Modelling of Buildings in Mixed Energy Distribution Systems*. PhD thesis, 2007.

[9] R. Billinton and R. Karki, "Capacity expansion of small isolated power systems using pv and wind energy," *IEEE Power Engineering Review*, vol. 21, no. 10, pp. 62–62, 2001.

[10] M. Kaltschmitt, W. Streicher, and A. Wiese, *Basics of Renewable Energy Supply*. Springer Berlin Heidelberg, 2007.

[11] L. Narvarte and E. Lorenzo, "Tracking and ground cover ratio," *Progress in Photovoltaics: Research and Applications*, vol. 16, no. 8, pp. 703–714, 2008.

[12] W. C. Dickinson, P. N. Cheremisinoff, and I. S. E. Society., *Solar energy technology handbook / editors, William C. Dickinson, Paul N. Cheremisinoff ; sponsored by American Section of the International Solar Energy Society, inc.* M. Dekker, New York :, 1980.

[13] B. Y. H. Liu and R. C. Jordan, "Daily insolation on surfaces tilted toward the equator," *Trans. ASHRAE*, pp. 526–541, 1962.

[14] C. Spitters, H. Toussaint, and J. Goudriaan, "Separating the diffuse and direct component of global radiation and its implications for modeling canopy photosynthesis part i. components of incoming radiation," *Agricultural and Forest Meteorology*, vol. 38, no. 1-3, pp. 217 – 229, 1986.

[15] T. Ackermann, *Wind Power in Power Systems.* 2005.

[16] J. Manwell, J. McGowan, and A. Rogers, *Wind Energy Explained: Theory, Design and Application.* 2002.

[17] P. Katti and M. Khedkar, "Alternative energy facilities based on site matching and generation unit sizing for remote area power supply," *Renewable Energy*, vol. 32, no. 8, pp. 1346–1362, 2007.

[18] B. S. Borowy and Z. M. Salameh, "Methodology for optimally sizing the combination of a battery bank and pv array in a wind/pv hybrid system," *IEEE Transactions on Energy Conversion*, vol. 11, no. 2, pp. 367–375, 1996.

[19] R. Chedid and S. Rahman, "Unit sizing and control of hybrid wind-solar power systems," *IEEE Transactions on Energy Conversion*, vol. 12, no. 1, pp. 79–85, 1997.

[20] H. Melo and C. Heinrich, "Energy balance in a renewable energy community," in *Environment and Electrical Engineering (EEEIC), 2011 10th International Conference on*, pp. 1 –4, may 2011.

[21] H. Ibrahim, A. Ilinca, and J. Perron, "Energy storage systems - characteristics and comparisons," *Renewable and Sustainable Energy Reviews*, vol. 12, no. 5, pp. 1221 – 1250, 2008.

[22] "Mobiliteitsonderzoek nederland 2009," 2010.

[23] J. A. Pecas Lopes, F. J. Soares, P. M. Almeida, and M. Moreira da Silva, "Smart charging strategies for electric vehicles: Enhancing grid performance and maximizing the use of variable renewable energy resources," *EVS24 International Battery, Hybrid and Fuel Cell Electric Vehicle Symposium*, 2009.

Glossary

List of Acronyms

MW	megawatt
KNMI	Royal Netherlands Meteorological Institute
GCR	Ground Cover Ratio
DC	direct current
AC	alternating current
EV	Electric Vehicle
NiMH	Nickel Metal Hydride
Li-ion	Lithium ion
pu	per unit